



**Environmental  
Science**  
Processes & Impacts

**Assessing the Source of the Photochemical Formation of  
Hydroxylating Species from Dissolved Organic Matter Using  
Model Sensitizers**

Journal:	<i>Environmental Science: Processes &amp; Impacts</i>
Manuscript ID	EM-ART-08-2021-000345.R1
Article Type:	Paper

SCHOLARONE™  
Manuscripts

1  
2  
3 Environmental Significance Statement  
4

5 The photochemistry of DOM is of interest to environmental scientists. Photochemical reactions  
6 within DOM form a series of reactive intermediates, including hydroxylating species such as  
7  $\cdot\text{OH}$ . However, the formation pathway for these species continues to be an active area of  
8 research. Here, we explore the mechanism by which these species are formed. These results will  
9 support current efforts in the community to better understand DOM photochemistry.  
10  
11  
12  
13  
14  
15  
16  
17  
18  
19  
20  
21  
22  
23  
24  
25  
26  
27  
28  
29  
30  
31  
32  
33  
34  
35  
36  
37  
38  
39  
40  
41  
42  
43  
44  
45  
46  
47  
48  
49  
50  
51  
52  
53  
54  
55  
56  
57  
58  
59  
60

1  
2  
3  
4 1           **Assessing the Source of the Photochemical Formation of**  
5  
6  
7 2           **Hydroxylating Species from Dissolved Organic Matter Using Model**  
8  
9  
10 3                           **Sensitizers**

11  
12 4           Kylie Couch<sup>1</sup>, Frank Leresche<sup>1</sup>, Claire Farmer<sup>1</sup>, Garrett McKay<sup>2,\*</sup>, and Fernando L.  
13  
14  
15 5                           Rosario-Ortiz<sup>1,\*</sup>

16  
17 6           <sup>1</sup> Department of Civil, Environmental, and Architectural Engineering, Environmental  
18  
19 7           Engineering Program, 607 UCB, University of Colorado Boulder, CO 80309, USA

20  
21 8           <sup>2</sup> Zachry Department of Civil and Environmental Engineering, 3136 TAMU, Texas  
22  
23  
24 9                           A&M University, College Station, TX 77843

25  
26  
27 10  
28  
29  
30 11           \* Corresponding authors: gmckay@tamu.edu; Fernando.rosario@colorado.edu  
31  
32  
33  
34  
35  
36  
37  
38  
39  
40  
41  
42  
43  
44  
45  
46  
47  
48  
49  
50  
51  
52  
53  
54  
55  
56  
57  
58  
59  
60

1  
2  
3 12 **ABSTRACT**  
4

5 13 Dissolved organic matter (DOM) is ubiquitous in natural waters and can facilitate the  
6  
7 14 chemical transformation of many contaminants through the photochemical production of reactive  
8  
9 15 intermediates, such as singlet oxygen ( $^1\text{O}_2$ ), excited triplet state DOM ( $^3\text{DOM}^*$ ), and  
10  
11 16 hydroxylating species ( $^{\bullet}\text{OH}$  and other intermediates of similar reaction chemistry). The formation  
12  
13 17 mechanism of most reactive intermediates is well understood, but this is not the case for the  
14  
15 18 formation of hydroxylating species from DOM. To investigate this chemistry, DOM model  
16  
17 19 sensitizers were irradiated with two different probe compounds (benzene and benzoic acid) at  
18  
19 20 two irradiation wavelengths (254 and 320 nm). The ability of DOM model sensitizers to  
20  
21 21 hydroxylate these arene probes was assessed by measuring rates of formation of the  
22  
23 22 hydroxylated probe compounds (phenol and salicylic acid). Multiple classes of model sensitizers  
24  
25 23 were tested, including quinones, hydroxybenzoic acids, aromatic ketones, and other triplet  
26  
27 24 forming species. Of these classes of model sensitizers, only quinones and hydroxybenzoic acids  
28  
29 25 had a hydroxylating capacity. Methanol quenching experiments were used to assess the reactivity  
30  
31 26 of hydroxylating species. These results have several implications for the systems tested. First,  
32  
33 27 they suggest that the hydroxylating intermediate produced from hydroxybenzoic acid photolysis  
34  
35 28 may not be hydroxyl radical, but a different hydroxylating species. Also, these data prompted  
36  
37 29 investigation of whether quinone photoproducts have a hydroxylating capacity. These results  
38  
39 30 confirm that hydroxybenzoic acids and quinones are important to the photochemical production  
40  
41 31 of hydroxylating species from DOM, but the mechanism by which this occurs for these classes of  
42  
43 32 sensitizers is still elusive.  
44  
45  
46  
47  
48  
49  
50  
51  
52  
53  
54  
55  
56  
57  
58  
59  
60

## 33 INTRODUCTION

34 Dissolved organic matter (DOM) is the primary light absorbing species in natural waters  
35 and has been shown to facilitate the chemical transformation of various contaminants through the  
36 production of reactive intermediates (RI).<sup>1-5</sup> These RI, which include singlet oxygen (<sup>1</sup>O<sub>2</sub>),  
37 excited triplet state DOM (<sup>3</sup>DOM\*), and hydroxylating species (\*OH and other intermediates of  
38 similar reaction chemistry), can react with many contaminants, making them important  
39 participants in the photodegradation of contaminants in natural waters and in engineered  
40 systems.<sup>6-12</sup>

41 The formation mechanisms for most RI are well understood,<sup>10; 13; 14</sup> however, this is not  
42 the case for the formation of hydroxylating species from DOM. DOM photohydroxylation  
43 mechanisms can be differentiated experimentally by the involvement (or lack thereof) of  
44 hydrogen peroxide and/or dissolved oxygen.<sup>2</sup> The H<sub>2</sub>O<sub>2</sub>-dependent pathway involves Fenton-like  
45 reactions<sup>1; 15; 16</sup> and results in the direct formation of \*OH, whereas the H<sub>2</sub>O<sub>2</sub>-independent  
46 pathway involves the production of hydroxylating species directly through photochemical  
47 reactions involving DOM. The precise mechanism by which hydroxylating species are produced  
48 from DOM photolysis (H<sub>2</sub>O<sub>2</sub>-independent pathway) has remained elusive, both in terms of the  
49 chemical moieties involved and identity of the oxidant. Although early studies attributed DOM  
50 photohydroxylation reactions to \*OH,<sup>2; 17</sup> a study by Page et al.<sup>18</sup> suggested that the production of  
51 hydroxylating species from DOM photolysis may not exclusively be \*OH, prompting the  
52 acknowledgement of yet-unknown hydroxylating species that are also formed through  
53 photochemical reactions of DOM. These so-called \*OH-like species have been invoked,<sup>19-21</sup>  
54 which have lower, but not well-defined, reactivity compared to \*OH.<sup>21</sup> A primary difficulty in

1  
2  
3 55 teasing apart the role of  $\cdot\text{OH}$  versus so-called  $\cdot\text{OH}$ -like species is that photohydroxylation  
4  
5 56 reactions of many organic molecules result in identical products.<sup>13</sup>  
6  
7

8 57 The identity of  $\cdot\text{OH}$ -like species is somewhat ambiguous, but the current understanding is  
9  
10 58 that these species are either excited states or excited state complexes of chromophores within  
11  
12 59 DOM. Previous studies have employed model sensitizers to assess potential mechanisms for the  
13  
14 60  $\text{H}_2\text{O}_2$ -independent pathway by which  $\cdot\text{OH}$ -like species are produced.<sup>10; 19; 21-25</sup> These sensitizers  
15  
16 61 are selected based on their presence in DOM (e.g. quinones, aromatic ketones, aromatic acids)  
17  
18 62 and whether they are photochemically active. Even if these groups are part of larger molecular  
19  
20 63 weight structures, it is believed that the use of the model sensitizers is still warranted as it could  
21  
22 64 be expected that these functionalities will still represent the primary photochemically active part  
23  
24 65 of DOM. Notably, DOM absorbance can be interpreted using a superposition model or a charge-  
25  
26 66 transfer model.<sup>26</sup> The use of individual model sensitizers invokes the superposition model, which  
27  
28 67 is justified in this study because the irradiation wavelengths chosen (254 and 320 nm) excite  
29  
30 68 local states, not charge transfer states, which are hypothesized to occur mainly at 350 nm  
31  
32 69 excitation or longer.<sup>27</sup> Also, it should be noted that recent studies<sup>28; 29</sup> have shown that charge-  
33  
34 70 transfer transitions may not be as prevalent as originally hypothesized.<sup>27</sup>  
35  
36  
37  
38  
39

40 71 Similar to other RI,  $\cdot\text{OH}$  and other hydroxylating species can be quantified using probe  
41  
42 72 compounds.<sup>13; 30</sup> Some probe compounds that have been used for the detection of hydroxylating  
43  
44 73 species from DOM photolysis are dimethyl sulfoxide, methane, benzene, nitrobenzene, benzoic  
45  
46 74 acid, *p*-chlorobenzoic acid, and terephthalic acid.<sup>13; 19; 23; 31-33</sup> These probe compounds react  
47  
48 75 either by hydrogen atom abstraction (e.g., methane) or hydroxylation (e.g. DMSO, arenes).<sup>13</sup>  
49  
50 76 Ideally, probe compounds are selective for reaction with  $\cdot\text{OH}$  or  $\cdot\text{OH}$ -like species, but there is  
51  
52 77 evidence that  $\cdot\text{OH}$ -like species react with some probe compounds in a way that is  
53  
54  
55  
56  
57  
58  
59  
60

1  
2  
3 78 indistinguishable from  $\cdot\text{OH}$  reaction.<sup>18; 20; 21</sup> Due to their lack of selectivity, most probe  
4  
5 79 compounds measure the hydroxylating capacity of a given system, which encompasses the  
6  
7 80 measurement of both  $\cdot\text{OH}$  and other hydroxylating species. Methane is the only probe thought to  
8  
9 81 be selective for  $\cdot\text{OH}$ , due to its high H-C bond dissociation energy. For this reason, methane has  
10  
11 82 been used to distinguish between  $\cdot\text{OH}$  and  $\cdot\text{OH}$ -like species,<sup>18; 19</sup> but its use also has practical  
12  
13 83 limitations, such as a limited solubility and existing as a gas at room temperature.  
14  
15  
16

17 84         Some sensitizers that have been shown to produce hydroxylating species upon irradiation  
18  
19 85 include quinones and hydroxybenzoic acids.<sup>19; 21; 22; 32; 34</sup> Early studies of the photochemical  
20  
21 86 production of a hydroxylating intermediate from quinones utilized a spin trap probe, 5,5-  
22  
23 87 dimethyl-1-pyrroline-1-oxide (DMPO).<sup>32; 34-36</sup> These studies claimed that the  $\cdot\text{OH}$  is formed via  
24  
25 88 H-atom abstraction when triplet quinones react with water. However, a number of studies have  
26  
27 89 shown that there are other photochemical pathways that occur in the presence of triplet quinones  
28  
29 90 that yield the same product as the reaction between DMPO and  $\cdot\text{OH}$ .<sup>37-39</sup> For this reason,  
30  
31 91 conclusions from earlier studies that utilized DMPO as probe compound are not reliable. Other  
32  
33 92 studies have been performed using dimethyl sulfoxide (DMSO) as a probe compound to assess  
34  
35 93 the chemical behavior of the hydroxylating intermediate produced from 2-methyl-*p*-  
36  
37 94 benzoquinone photolysis by measuring the production of methyl radicals from the reaction of the  
38  
39 95 hydroxylating intermediate with DMSO.<sup>19; 21</sup> However, a few studies have presented data that  
40  
41 96 brings into question the use of DMSO as a probe for hydroxylating species.<sup>39; 40</sup> Von Sonntag et  
42  
43 97 al. tested DMSO as a probe for hydroxylating species produced from *p*-benzoquinone photolysis  
44  
45 98 and did not detect methyl radicals, suggesting that there is no oxidizing intermediate and that *p*-  
46  
47 99 benzoquinone undergoes direct photodegradation for form its photoproducts.<sup>39</sup> Interestingly,  
48  
49 100 Gerner utilized DMSO as a probe and did observe the production of methyl radical, but  
50  
51  
52  
53  
54  
55  
56  
57  
58  
59  
60

1  
2  
3 101 attributed it to the reaction of the triplet quinone with DMSO.<sup>40</sup> This contradictory data makes  
4  
5 102 DMSO a questionable probe compound and is the reason DMSO was not used in this study.  
6  
7  
8 103 Additionally, Gan et al. used methane as a probe and established that the hydroxylating  
9  
10 104 intermediate produced from 2-methyl-*p*-benzoquinone photolysis is not  $\cdot\text{OH}$ .<sup>19</sup> The same study  
11  
12 105 hypothesized that the unknown hydroxylating intermediate is a quinone–water exciplex. Overall,  
13  
14 106 the identity of the hydroxylating species produced from quinone photolysis and the mechanism  
15  
16 107 by which this happens are still in question. Considering hydroxybenzoic acids, one previous  
17  
18 108 study that utilized benzene and methane as a probe and quencher, respectively, concluded that  
19  
20 109 this class of sensitizers produces  $\cdot\text{OH}$  when photolyzed at wavelengths between 290 and 330  
21  
22 110 nm.<sup>22</sup> This study suggested that, among other possible mechanisms, photooxidation followed by  
23  
24 111 water addition and subsequent  $\cdot\text{OH}$  cleavage may produce  $\cdot\text{OH}$ .<sup>22</sup>  
25  
26  
27

28 112 The production of hydroxylating species from DOM photolysis in surface waters and  
29  
30 113 engineered systems is important because these chemical species can facilitate the transformation  
31  
32 114 of contaminants. Assessing the reactivity of  $\cdot\text{OH}$ -like species and how it differs from that of  $\cdot\text{OH}$   
33  
34 115 is key for understanding and predicting the degradation pathways of chemical contaminants in  
35  
36 116 water. This study focused on three objectives. First, the production of hydroxylating species  
37  
38 117 during photolysis of various classes of model sensitizers was investigated. Second, the possibility  
39  
40 118 that different mechanisms are responsible for this hydroxylating capacity was assessed by  
41  
42 119 utilizing different arene probe compounds and methanol as a quencher. Third, apparent quantum  
43  
44 120 yields of hydroxylated probe compound formation from the sensitizers in this study were  
45  
46 121 compared to apparent  $\cdot\text{OH}$  quantum yields from DOM photolysis. Overall, this work contributes  
47  
48 122 to a larger understanding of the photochemistry of DOM in natural waters and engineered  
49  
50 123 systems as it applies to the fate and transport of contaminants.  
51  
52  
53  
54  
55  
56  
57  
58  
59  
60



## 124 MATERIALS AND METHODS

### 125 *Selection of Model Sensitizers*

126 Sensitizers were selected to include chemical species that have been shown to produce  
127 hydroxylating species upon photolysis, such as quinones<sup>19; 21; 41; 42</sup> and hydroxybenzoic acids.<sup>43</sup>  
128 Additional compounds were selected as a negative control that exhibit triplet state  
129 photochemistry but were not expected to produce hydroxylating species. Model sensitizers  
130 selected include *p*-benzoquinone (PBQ), anthraquinone-2-sulfonic acid (A2S), 2,6-dimethoxy-*p*-  
131 benzoquinone (DPBQ), 4-hydroxybenzoic acid (4HBA), 2,4-dihydroxybenzoic acid (DHBA),  
132 umbelliferone (UMI), *trans*-cinnamic acid (TCA), 4-benzoylbenzoic acid (4BA), and 3-  
133 methoxyacetophenone (3MP). All sensitizers structures are presented in Figure 1 with their  
134 corresponding triplet state energy and triplet state one electron reduction potentials. Although  
135 A2S may not be the best model for quinone structures in DOM because of its reactivity towards  
136 phenol (the product of benzene hydroxylation), it was selected because previous studies have  
137 used this compound to explore quinone photochemistry and model DOM photochemistry.<sup>23; 34; 44</sup>

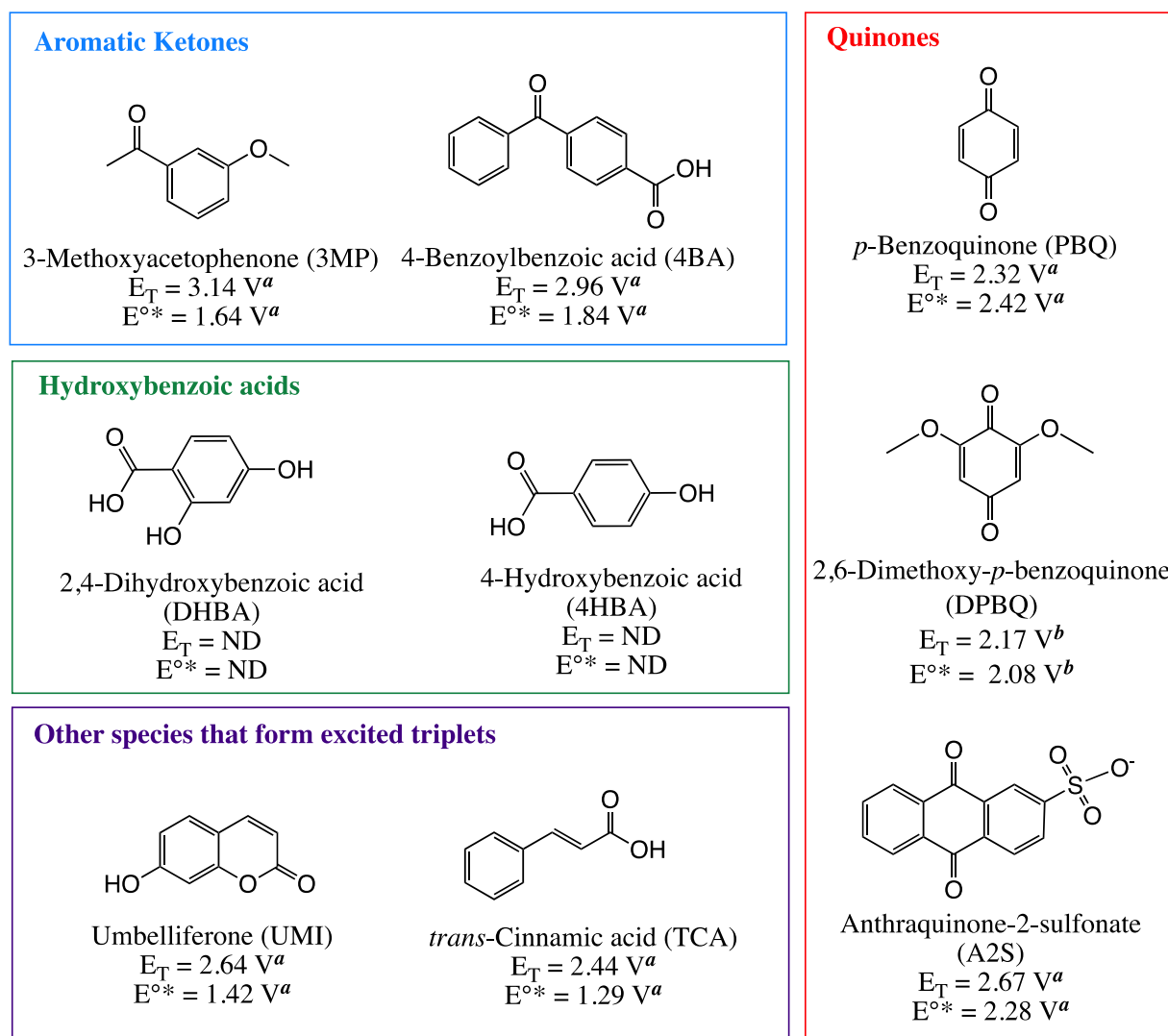
### 138 *Chemicals and solutions*

139 All chemicals were purchased from commercial sources and are listed in the Electronic  
140 Supplementary Information (ESI) Table S1 with their respective CAS numbers and purities.  
141 Hydrogen peroxide, nitrate, and nitrite were used as sources of  $\cdot\text{OH}$ . Solutions were prepared in  
142 MilliQ water, with the pH adjusted to  $7.0 \pm 0.1$  using sodium hydroxide ( $\sim 20$  mM). Samples  
143 were not prepared in buffers to avoid complicating the chemistry of the hydroxylating  
144 intermediates, which has been observed in systems containing *p*-benzoquinone in which the  
145 triplet *p*-benzoquinone reacts with phosphate to form an intermediate, *p*-benzoquinone-2-  
146 phosphate.<sup>39</sup> During experiments performed with unbuffered solutions there was approximately

1  
2  
3 147 0.5 unit decrease in pH from the original pH of  $7.0 \pm 0.1$ . All model sensitizers besides UMI  
4  
5 148 (pKa  $\sim 7.8$ ) would be unaffected by this pH change. In the case of UMI, a decrease in 0.5 pH  
6  
7 149 units would change the fraction of deprotonated species from 0.13 to 0.044.  
8  
9

### 10 150 *Quantification of hydroxylating species*

11  
12 151 Many probe compounds are available for detection of hydroxylating species, but probes  
13  
14 152 relying on aromatic ring hydroxylation are among the most widely used in the aquatic  
15  
16 153 photochemistry community.<sup>20; 22; 23; 31</sup> This was the main motivation for the choice of probes in  
17  
18 154 this study, which were benzene and benzoic acid. Exploration of the chemistry of hydroxylating  
19  
20 155 species with these two aromatic probes is important because of the frequency with which they  
21  
22 156 are used to study the production of hydroxylating species from DOM. These results are  
23  
24 157 important to previous studies that employ benzene or benzoic acid as probes for the production  
25  
26 158 of hydroxylating species from DOM photolysis. The formation of hydroxylating species was  
27  
28 159 detected by monitoring the hydroxylated product of the reaction between the probe compound  
29  
30 160 and hydroxylating species. In the cases of benzoic acid and benzene, the formation of salicylic  
31  
32 161 acid and phenol were monitored, respectively. Rate constants for quenching of  $\cdot\text{OH}$  with benzene  
33  
34 162 and benzoate are  $7.8 \times 10^9$  and  $5.9 \times 10^9 \text{ M}^{-1} \text{ s}^{-1}$ , respectively.<sup>7</sup> It should be noted that we used  
35  
36 163 benzene and benzoate as high concentration probes,<sup>13</sup> i.e., the majority ( $\geq 97\%$ ) of  $\cdot\text{OH}$  produced  
37  
38 164 reacted with benzene or benzoate (except for the experiments conducted in the presence of  
39  
40 165 methanol as a quencher where the fraction of  $\cdot\text{OH}$  produced reacting with the probe can be  
41  
42 166 calculated using eq. 5, see below).  
43  
44  
45  
46  
47  
48  
49  
50  
51  
52  
53  
54  
55  
56  
57  
58  
59  
60



167

168 **Figure 1.** Model sensitizers used in this study, their structures, triplet state one electron reduction  
 169 potentials ( $E^{\circ*}$ ), and triplet energies ( $E_T$ ). ND = No Data, <sup>a</sup>McNeill and Canonica,<sup>10</sup> <sup>b</sup>Vaughan et  
 170 al.<sup>2</sup>

171

### 172 *Analytical instrumentation*

173 Analysis of salicylic acid and phenol was performed with an Agilent 1200 Series high  
 174 performance liquid chromatography (HPLC) equipped with an Eclipse Plus XDB-C18 column  
 175 with  $4.6 \times 150$  mm dimensions and  $5 \mu\text{m}$  particle size. The salicylic acid method employed an  
 176 isocratic mobile phase of 30% acetonitrile and 70% pH 2.8, 10 mM  $\text{H}_3\text{PO}_4$  with a flow rate of  
 177  $1.0 \text{ mL min}^{-1}$ . Analytes were using a fluorescence detector with excitation and emission

1  
2  
3 178 wavelengths set to 320 nm and 410 nm, respectively. The typical retention time of salicylic acid  
4  
5 179 in the system was approximately 6 min. The phenol method employed an isocratic mobile phase  
6  
7  
8 180 of 30% acetonitrile and 70% pH 2.8, 10 mM H<sub>3</sub>PO<sub>4</sub> with a flow rate of 1.0 mL min<sup>-1</sup>. Phenol was  
9  
10 181 quantified using a fluorescence detector with excitation and emission wavelengths set to 260 nm  
11  
12 182 and 310 nm, respectively. The typical retention time of phenol in the system was approximately  
13  
14  
15 183 5 min. Limit of quantification determined by the signal/noise method for phenol and salicylic  
16  
17 184 acid were of 6 nM for both methods.

### 185 *Irradiation experiments*

186 A Rayonet RPR-100 (Southern New England Ultraviolet Company) was used for  
187 irradiations, employing either 254 or 320 nm lamps. The samples were placed in ≈9mL  
188 stoppered quartz tubes (diameter 1.25cm) on a carousel rotating in the center of the photoreactor  
189 and were irradiated from the side. The 254 nm lamps emit light ranging from 249 nm to 258 nm.  
190 Quantum yield calculations for experiments using 254 nm lamps were treated as monochromatic.  
191 The 320 lamps emit light broadly centered around 313nm (270-350nm), with secondary emission  
192 peak extending up to 400 nm. Quantum yield calculations for experiments using 320 nm lamps  
193 were treated as polychromatic. Lamp spectra overlaid with absorption spectra of the sensitizers  
194 can be found in the ESI, Figure S1. The Rayonet RPR-100 employs a fan to control temperature.  
195 Photon irradiance was quantified daily using chemical actinometry: Uridine actinometry was  
196 used for 254 nm irradiations<sup>45</sup> and *p*-nitroanisole/pyridine (PNA/PYR) actinometry was used for  
197 320 nm irradiations.<sup>46</sup> More information about actinometry procedure can be found in ESI Text  
198 S1. Irradiance spectra of the lamps were collected using a spectroradiometer and can be found in  
199 the ESI, Figures S1 and S2.

1  
 2  
 3 200 Irradiation experiments at 254 nm were performed with 1 mM benzoic acid as the probe  
 4  
 5 201 compound and experiments at 320 nm were performed using 3 mM benzene as the probe  
 6  
 7 202 compound. At these concentrations the probe compounds act as rate of formation probes,  
 8  
 9 203 rendering the fraction of conversion of the probes to be negligible. For experiments performed  
 10  
 11 204 using 254 nm lamps the concentration of sensitizers was adjusted to be optically matched at an  
 12  
 13 205 initial optical density of 0.3. Concentrations of sensitizers in experiments normalizing  
 14  
 15 206 absorbance to 0.3 ranged from approximately 10 – 100  $\mu\text{M}$ . The total absorbance of these  
 16  
 17 207 experimental solutions, including benzoic acid, was 0.83, leaving the sensitizers accounting for  
 18  
 19 208 ~37% of the light absorbed by the experimental solutions. For 254 nm experiments, solution  
 20  
 21 209 temperature was not controlled due to the short irradiation times required with little temperature  
 22  
 23 210 variation, between 23 and 28  $^{\circ}\text{C}$ . For experiments performed using 320 nm lamps, sensitizers  
 24  
 25 211 concentrations were 20  $\mu\text{M}$ . Longer irradiation times were required for 320 nm experiments and  
 26  
 27 212 a shift in temperature was observed as a result of longer irradiation time. For this reason, prior to  
 28  
 29 213 experimentation the solution temperature was adjusted to  $30 \pm 3$   $^{\circ}\text{C}$  using a water-jacketed petri  
 30  
 31 214 dish, which is the steady-state temperature of the photochemical reactor.

32  
 33 215 Two corrections were made to experimental data. First, because benzoic acid absorbs  
 34  
 35 216 strongly at 254 nm (Figure S2), the light screening factor for these experimental solutions was  
 36  
 37 217 calculated and quantum yields were corrected for light screening following the procedure by  
 38  
 39 218 Wenk et al.<sup>4</sup> The equation used for these calculations is as follows,

$$S_{\lambda,PC,Sens} = \frac{1 - e^{-2.303(\epsilon_{\lambda,PC}[PC] + \epsilon_{\lambda,Sens}[Sens])l}}{2.303(\epsilon_{\lambda,PC}[PC] + \epsilon_{\lambda,Sens}[Sens])l} \quad (1)$$

40  
 41 219 where  $\epsilon_{\lambda,PC}$  and  $\epsilon_{\lambda,Sens}$  are the molar extinction coefficients for the PC and sensitizers in  $\text{M}^{-1} \text{cm}^{-1}$   
 42  
 43 220 and [PC] and [Sens] are the concentrations of PC and sensitizers in M. This resulted in a light  
 44  
 45 221 screening factor of 0.43 applied to all solutions containing sensitizers normalized to absorbance

1  
2  
3 222 of 0.3. Using benzene with the 320 nm lamps did not present the same issue, as benzene does not  
4  
5 223 absorb strongly in the wavelength range emitted by these lamps, shown in ESI Figure S2.  
6  
7  
8 224 Second, for all experiments with sensitizers, rates of formation of the hydroxylated probe  
9  
10 225 compound were corrected for formation of the hydroxylated probe compound from the direct  
11  
12 226 photolysis of the probe compound itself. Additionally, control experiments were performed with  
13  
14 227 DHBA to determine whether direct photolysis of DHBA results in salicylic acid, chromatograms  
15  
16  
17 228 for HPLC analysis of these experimental solutions are shown in ESI Figure S3. This data shows  
18  
19 229 that the direct photolysis of DHBA does not produce salicylic acid and, therefore, will not affect  
20  
21 230 the quantum yield results. For the experiments using 4HBA as photosensitizer and benzoate as  
22  
23  
24 231 the hydroxylating species probe, one consideration is that 4HBA is itself one of the reaction  
25  
26 232 products between benzoate and hydroxylating species.<sup>47</sup> As 4HBA concentration decreased  
27  
28 233 during irradiation (Figure S5) we conclude that 4HBA formation from benzoate hydroxylation  
29  
30  
31 234 can be safely neglected in the experiments analysis.  
32

33 235 It is important to note that experimental limitations required use of different probe  
34  
35 236 compound at 254 nm and 320 nm irradiation. Specifically, salicylic acid absorbs in the  
36  
37 237 wavelength range emitted by the 320 nm lamps (Figure S2) and undergoes non-negligible direct  
38  
39 238 photolysis (Figure S4), which precluded use of 320 nm lamps with benzoic acid as a probe  
40  
41  
42 239 compound. At 254 nm, benzoic acid screens most of the incoming light, minimizing direct  
43  
44 240 photolysis of the salicylic acid photoproduct. The hydroxylated product of benzene (phenol) does  
45  
46  
47 241 not absorb at 320 nm (Figure S2). For all experiments with sensitizers, rates of formation of the  
48  
49 242 hydroxylated probe compound were corrected for the production of the hydroxylated probe  
50  
51 243 compound from the direct photolysis of the probe compound itself.  
52  
53  
54  
55  
56  
57  
58  
59  
60

1  
2  
3 244 Methanol was added as a quencher in some experiments to assess whether the  $\cdot\text{OH}$ -like  
4  
5 245 species reacts with methanol similarly to  $\cdot\text{OH}$ . In these experiments, methanol was spiked into  
6  
7  
8 246 solutions prior to irradiation at concentrations ranging between 0 and 0.1 M. Methanol reacts  
9  
10 247 with  $\cdot\text{OH}$  with a second-order reaction rate constant of  $9.7 \times 10^8 \text{ M}^{-1} \text{ s}^{-1}$ .<sup>7</sup> It is hypothesized that  
11  
12 248 the reaction between methanol and other hydroxylating species to be different than that of  $\cdot\text{OH}$   
13  
14  
15 249 because hydroxyl radicals are non-selective and react with many molecules at near diffusion-  
16  
17 250 controlled rates. A similar method was used in a study of DOM photochemistry by Leresche et  
18  
19 251 al.<sup>48</sup>

21 252 Reaction pathways involving methanol or triplet quinones have been shown to produce  
22  
23  
24 253 superoxide, a fraction of which will dismutate to  $\text{H}_2\text{O}_2$ , which can undergo direct photolysis to  
25  
26 254 form  $\cdot\text{OH}$ .<sup>49-52</sup> Calculations were performed to estimate the rate of formation of  $\cdot\text{OH}$  from these  
27  
28  
29 255 pathways considering both 254 and 320 nm irradiation (see ESI Text S2), the highest resulting  
30  
31 256 values being on an order of  $10^{-12} \text{ M s}^{-1}$  with specific values varying based on the concentration of  
32  
33 257  $\text{H}_2\text{O}_2$ . This value is  $\sim 2 - 3$  orders of magnitude lower than the rates of hydroxylated probe  
34  
35  
36 258 compound formation observed in this study (ESI Table S3). Based on these calculations,  $\text{H}_2\text{O}_2$  is  
37  
38 259 not expected to contribute significantly to observed rates of formation of hydroxylated probe  
39  
40 260 compounds.

### 41 42 261 *Quantum Yield Analysis*

43  
44  
45 262 In order to compare the photoreactivity of sensitizers, apparent  $\cdot\text{OH}$  quantum yields were  
46  
47 263 calculated. Quantum yields were calculated for both sensitizer/wavelength systems: benzoic acid  
48  
49 264 with 254 nm light and benzene with 320 nm light. Apparent quantum yields were calculated as  
50  
51  
52 265 described by (eq. 2)

$$\Phi_{\text{OH}} = \frac{R_{\bullet\text{OH}}}{k_{\text{Sens} - a}[\text{Sens}]} \quad (2)$$

266 where  $R_{\bullet\text{OH}}$  is the rate of formation of hydroxylating species in  $\text{M s}^{-1}$ ,  $k_{\text{Sens} - a}$  the specific rate of  
 267 light absorption by sensitizers in  $\text{s}^{-1}$ , and  $[\text{Sens}]$  is the sensitizer's concentration in  $\text{M}$ . The  
 268 specific rate of light absorption of sensitizers was calculated using eq. 3.

$$k_{\text{Sens} - a} = 1000E_{\text{p,total}}^0 \sum_{\lambda} \frac{\rho_{\lambda} \varepsilon_{\text{Sens}}(\lambda) (1 - 10^{-(\varepsilon_{\text{Sens}}(\lambda)[\text{Sens}] + \varepsilon_{\text{PC}}(\lambda)[\text{PC}]l})}{(\varepsilon_{\text{Sens}}(\lambda)[\text{Sens}] + \varepsilon_{\text{PC}}(\lambda)[\text{PC}]l)} \quad (3)$$

269 In eq. 3,  $E_{\text{p,total}}^0$  is the photon irradiance of the Rayonet photoreactor in  $\text{Einstein cm}^{-2} \text{s}^{-1}$ ,  $\rho_{\lambda}$  the  
 270 relative spectral photon irradiance,  $\varepsilon_{\text{Sens}}(\lambda)$  the molar absorption coefficient at the wavelength  $\lambda$   
 271 of the sensitizers in  $\text{M}^{-1} \text{cm}^{-1}$ ,  $\varepsilon_{\text{PC}}(\lambda)$  the molar absorption coefficient at the wavelength  $\lambda$  of the  
 272 probe compound in  $\text{M}^{-1} \text{cm}^{-1}$ ,  $[\text{PC}]$  the concentration of the probe compound in  $\text{M}$ , and  $l$  the  
 273 optical pathlength in  $\text{cm}$ . Additionally,  $R_{\bullet\text{OH}}$  is defined as follows,

$$R_{\bullet\text{OH}} = \frac{R_{\text{PC} - \text{OH}}}{Y_{\bullet\text{OH}}} \quad (4)$$

274 where  $R_{\text{PC} - \text{OH}}$  is the rate of formation of the hydroxylated probe compound and  $Y_{\bullet\text{OH}}$  the yield  
 275 for the reaction of  $\bullet\text{OH}$  with the probe compound.

276 The yield for the reaction of other hydroxylating species with the probe compound,  
 277  $Y_{\bullet\text{OH} - \text{like}}$ , is unknown, so for these calculations,  $Y_{\bullet\text{OH}}$  was used for all sensitizers. A reasonable  
 278 hypothesis about whether  $Y_{\bullet\text{OH} - \text{like}}$  is less than or greater than  $Y_{\bullet\text{OH}}$  cannot be made without  
 279 more information about the identity of the  $\bullet\text{OH}$ -like intermediate and the mechanism by which it  
 280 reacts with probe compounds. Additionally, this difference is difficult to quantitatively constrain  
 281 due to the unknown quantum yield for the production of other hydroxylating species from  
 282 sensitizers (apart from the use of probe compounds). Therefore, the quantum yields calculated in  
 283 this study simply use  $Y_{\bullet\text{OH}}$  as a benchmark for the expected value of  $Y_{\bullet\text{OH} - \text{like}}$ . Even for  $\bullet\text{OH}$ , a



1  
2  
3 284 wide variety of yields exist in the literature for different arenes (e.g., ~0.3-0.9 for  $Y_{\bullet\text{OH}}$  of phenol  
4  
5  
6 285 from benzene), which may also be sensitive to solution conditions.<sup>53-57</sup>  $Y_{\bullet\text{OH}}$  for the reaction of  
7  
8 286  $\bullet\text{OH}$  with benzene to produce phenol, two more recent studies, Sun et al. and McKay and  
9  
10 287 Rosario-Ortiz, determined this yield to be  $0.693 \pm 0.022$  and  $0.63 \pm 0.07$ , respectively.<sup>20; 43</sup> These  
11  
12 288 values are in good agreement with each other and fall within the aforementioned range for this  
13  
14  
15 289 parameter. For this study the value determined by McKay and Rosario-Ortiz, which utilized  
16  
17 290 similar experimental conditions was used. Considering the formation salicylic acid from benzoic  
18  
19 291 acid hydroxylation, a  $Y_{\bullet\text{OH}}$  of 0.155 was used.<sup>58</sup>

### 292 *Methanol Quenching Model*

293 Methanol quenching was modeled by eq. 5, where  $f$  is the fraction of  $\bullet\text{OH}$  reacting with  
294 the probe compound.

$$f = \frac{k_{\text{PC},\bullet\text{OH}}[\text{PC}]}{k_{\text{MeOH},\bullet\text{OH}}[\text{MeOH}] + k_{\text{PC},\bullet\text{OH}}[\text{PC}] + k_{\text{Sens},\bullet\text{OH}}[\text{Sens}]} \quad (5)$$

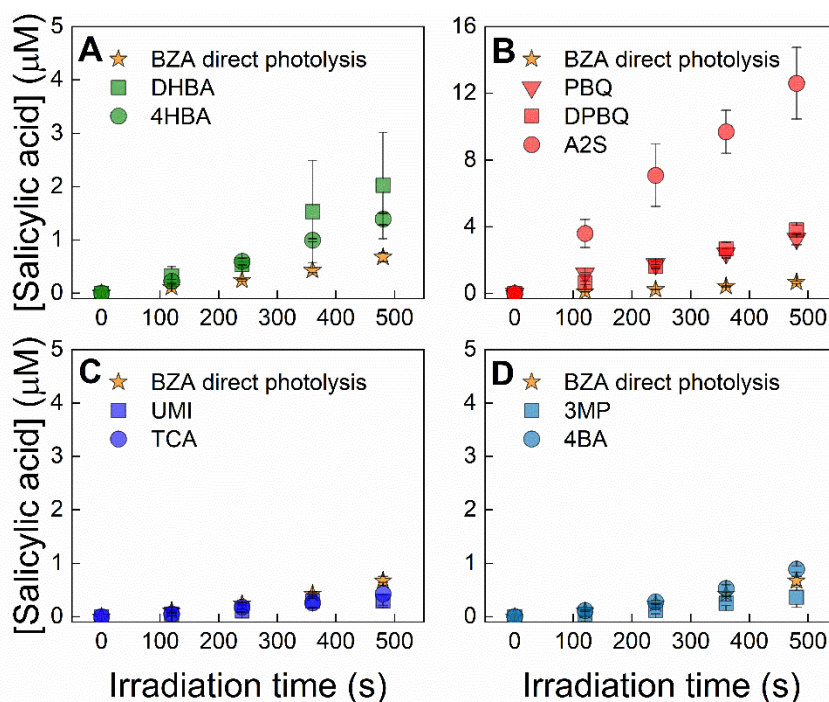
295 Where  $k_{\text{PC},\bullet\text{OH}}$ ,  $k_{\text{MeOH},\bullet\text{OH}}$ , and  $k_{\text{Sens},\bullet\text{OH}}$  are the second order rate constants for respectively the  
296 probe compound, sensitizers, and methanol (MeOH) with  $\bullet\text{OH}$  in  $\text{M}^{-1} \text{s}^{-1}$ , respectively. [PC],  
297 [Sens], and [MeOH] are the concentrations of respectively the probe compound, sensitizers, and  
298 MeOH in M.

## 299 **RESULTS**

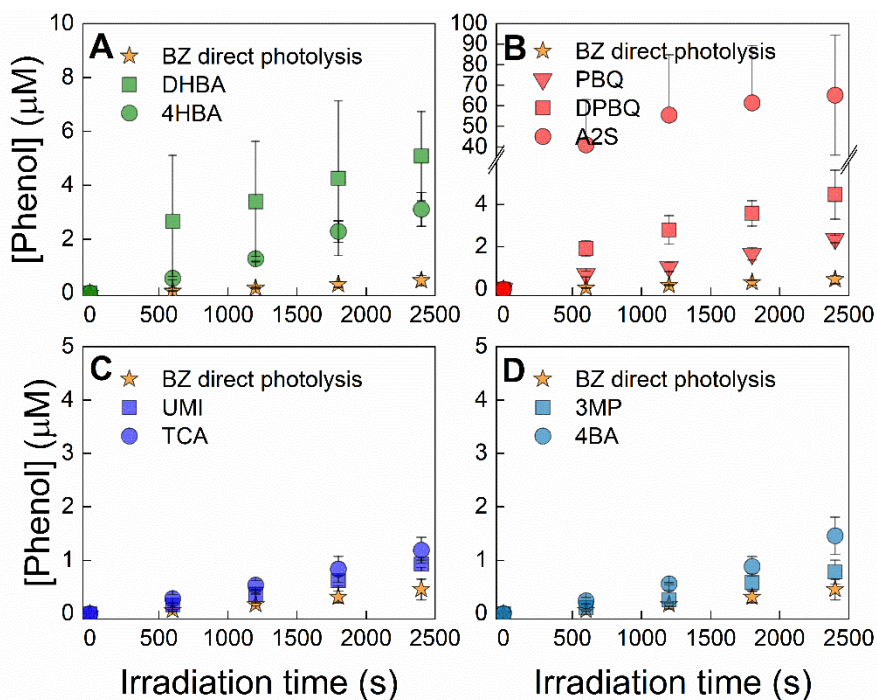
### 300 *Production of Hydroxylating Species from Model Sensitizers*

301 The formation of hydroxylating species ( $\bullet\text{OH}$  and  $\bullet\text{OH}$ -like species) from sensitizers was  
302 assessed using two different probe compounds with two irradiation wavelengths, benzoic acid  
303 with 254 nm irradiation and benzene with 320 nm irradiation. Figure 2 shows the results for the  
304 experiments performed using benzoic acid with 254 nm irradiation. Figure 3 shows results for

1  
2  
3 305 the experiments using benzene with 320 nm irradiation. Formation rates for the data in these  
4  
5 306 figures can be found in the ESI, Table S3. All samples were interpreted as linear with respect to  
6  
7 307 the formation of the hydroxylated probe compound with one exception: A2S with 320 nm  
8  
9 308 irradiation using benzene as the probe compound because the production of phenol is clearly  
10  
11 309 nonlinear (Figure 3). Direct photolysis controls revealed that benzoic acid photolysis produces  
12  
13 310 salicylic acid with a formation rate equal to  $1.4 \pm 0.08 \text{ nM s}^{-1}$ . Of the examined sensitizers,  
14  
15 311 irradiation of quinones and hydroxybenzoic acids produced greater rates of salicylic acid  
16  
17 312 formation ( $> 3.0 \text{ nM s}^{-1}$ ) than direct photolysis of benzoic acid, indicating that these sensitizers  
18  
19 313 have a hydroxylating capacity. Irradiation of quinones produced salicylic acid at rates between  
20  
21 314 5.9 and  $26 \text{ nM s}^{-1}$ , whereas irradiation of hydroxybenzoic acids produced salicylic acid at rates  
22  
23 315 between 3.0 and  $3.4 \text{ nM s}^{-1}$ . Conversely, the formation of salicylic acid in samples containing  
24  
25 316 aromatic ketones and other triplet forming species was within the range of the direct photolysis  
26  
27  
28  
29  
30  
31 317 control, suggesting that these sensitizers had a minimal hydroxylating capacity, if any.



319 **Figure 2.** Production of salicylic acid with respect to time from the photolysis of sensitizers in  
 320 the presence of 1 mM benzoic acid, irradiated with 254 nm lamps for 8 minutes. All samples  
 321 were adjusted to pH  $7.0 \pm 0.1$ . The concentration of sensitizers was adjusted to be optically  
 322 matched at an initial optical density of 0.3. Each subplot displays benzoic acid (BZA) direct  
 323 photolysis data. **A:** 2,4-Dihydroxybenzoic acid (DHBA), 4-Hydroxybenzoic acid (4HBA), **B:** *p*-  
 324 Benzoquinone (PBQ), 2,6-Dimethoxy-*p*-benzoquinone (DPBQ), Anthraquinone-2-sulfonate  
 325 (A2S), **C:** Umbelliferone (UMI), *trans*-Cinnamic acid (TCA), and **D:** 3-Methoxyacetophenone  
 326 (3MP), 4-Benzoylbenzoic acid (4BA).  
 327



328  
 329 **Figure 3.** Production of phenol with respect to time from the photolysis of 20  $\mu\text{M}$  sensitizers in  
 330 the presence of 3 mM benzene, irradiated with 320 nm lamps for 40 minutes. All samples were  
 331 adjusted to pH  $7.0 \pm 0.1$ . Each subplot displays benzene (BZ) direct photolysis data. **A:** 2,4-  
 332 Dihydroxybenzoic acid (DHBA), 4-Hydroxybenzoic acid (4HBA), **B:** *p*-Benzoquinone (PBQ),  
 333 2,6-Dimethoxy-*p*-benzoquinone (DPBQ), Anthraquinone-2-sulfonate (A2S), **C:** Umbelliferone  
 334 (UMI), *trans*-Cinnamic acid (TCA), and **D:** 3-Methoxyacetophenone (3MP), 4-Benzoylbenzoic  
 335 acid (4BA).

336 Similar to the results obtained with benzoic acid at 254 nm, direct photolysis of benzene  
 337 leads to its photohydroxylation, forming phenol ( $0.19 \pm 0.04 \text{ nM s}^{-1}$ , Table S3). As shown in  
 338 Figure 3 and ESI Table S3, all sensitizers irradiated at 320nm in the presence of benzene  
 339 produced phenol at rates greater than could be accounted for by direct photolysis alone (between  
 340 0.39 and  $2.2 \text{ nM s}^{-1}$ ). Quinone and hydroxybenzoic acid sensitizers had rates of phenol formation

1  
2  
3 341 sufficiently higher than that of the direct photolysis of benzene (all greater than  $0.95 \text{ nM s}^{-1}$ ),  
4  
5 342 compared to the results obtained for the aromatic ketones, umbelliferone, or trans-cinnamic acid  
6  
7 343 which were a maximum of  $0.41 \text{ nM s}^{-1}$  (for 4-benzoyl benzoic acid) greater than the rate of  
8  
9 344 formation from benzene. All samples, except those containing A2S, were interpreted as linear  
10  
11 345 with respect to the formation of phenol. In the case of A2S, the production of phenol was not  
12  
13 346 linear, and the formation rate was not included in ESI Table S3. This behavior can be attributed  
14  
15 347 to the reaction of triplet A2S with phenol, as it has been previously established that phenol is  
16  
17 348 oxidized by A2S.<sup>23</sup> DPBQ may be able to oxidize phenol, but the reaction does not appear to  
18  
19 349 occur significantly on the timeframe of the experiments. Leresche et al. observed a small (10%)  
20  
21 350 degradation of salicylic acid in irradiation experiments of DOM, which contains quinone  
22  
23 351 moieties, on a relatively longer timeframe (4 hours) than the condition used in the present  
24  
25 352 study.<sup>48</sup>

26  
27 353 Figure 3B shows that the yield of phenol from A2S photolysis is greater than the original  
28  
29 354 concentration of A2S in solution. There are a few possible explanations for this behavior. One  
30  
31 355 study found that the photodecomposition of anthraquinones is fully reversible in the presence of  
32  
33 356 oxygen while this is not true in the case of benzoquinones.<sup>59; 60</sup> This catalytic process could be  
34  
35 357 contributing to increased yields of hydroxylating species in the case of anthraquinones.  
36  
37 358 Additionally, some studies have observed an increase in the production of superoxide and  
38  
39 359 hydrogen peroxide from anthraquinone-2,6-disulfonate and 9,10-anthraquinone derivatives in the  
40  
41 360 presence of an electron donor.<sup>50; 61</sup> It is possible that benzene (which has an oxidation potential  
42  
43 361 of  $\sim 2.2 \text{ V}$ )<sup>62</sup> facilitates the catalytic production of hydrogen peroxide by continuously cycling  
44  
45 362 A2S between reduced ( $\text{A2S}^{\cdot-}$ ) and oxidized (A2S) states without forming other stable quinone  
46  
47 363 photoproducts. In the presence of an electron donor, if a high concentration of hydrogen peroxide  
48  
49  
50  
51  
52  
53  
54  
55  
56  
57  
58  
59  
60

1  
2  
3 364 is formed, an appreciable amount of  $\cdot\text{OH}$  could then be formed from hydrogen peroxide  
4  
5 365 photolysis. Ultimately, a combination of pathways that produce hydroxylating species are likely  
6  
7 366 contributing to the photochemical behavior of A2S that is observed in Figure 3B. Note that  
8  
9 367 phenol, the product of the reaction of benzene with hydroxylating species is itself an electron  
10  
11 368 donating species. A catalytical reaction of phenol with A2S would produce an exponential  
12  
13 369 formation of phenol vs time. As the opposite is observed (i.e., the formation rate of phenol is  
14  
15 370 decreasing with time), if the reaction of phenol with A2S is producing hydroxylating species its  
16  
17 371 overall yield should be  $\leq 1$ .

18  
19  
20  
21 372 Overall, the data presented in Figures 2 and 3 indicate that quinones and hydroxybenzoic  
22  
23 373 acids have a hydroxylating capacity. However, in contrast to the data from experiments using  
24  
25 374 benzoic acid with 254 nm irradiation (Figure 2), experiments using benzene with 320 nm  
26  
27 375 irradiation (Figure 3) show that the formation of phenol in systems containing aromatic ketones  
28  
29 376 and other triplet forming species may not entirely be attributed to the direct photolysis of  
30  
31 377 benzene. For the purposes of this study, aromatic ketones and other triplet forming species were  
32  
33 378 not investigated further because their formation rates were barely outside of the uncertainties for  
34  
35 379 the direct photolysis of benzene. Even if these sensitizers do participate in the production of  
36  
37 380 hydroxylating species, it is to a much lesser extent than quinones and hydroxybenzoic acids.

### 381 *Estimation of Quantum Yields for Model Sensitizers*

382 Quantum yields were calculated for sensitizers (Table 1), with values at 320 nm irradiation  
383 being considered apparent due to the lamp's polychromatic nature. There are two complicating  
384 factors for calculating the quantum yields for the sensitizers. First, because the yields of  
385 hydroxylated probe compound from the reaction of hydroxylating species other than  $\cdot\text{OH}$  are  
386 unknown, the yield for the reaction of the probe compound with  $\cdot\text{OH}$  ( $Y_{\cdot\text{OH}}$ ) was used. It is

387 expected that the reaction rate constants of these  $\cdot\text{OH}$ -like species are different than that of  $\cdot\text{OH}$ ,  
 388 which reacts with benzene and benzoic acid at near diffusion-controlled rates.<sup>7</sup> For this reason,  
 389 the data in Table 1 can be treated as estimates of the true quantum yield for these systems. Even  
 390 given the uncertainty in yield, there is a benefit to presenting the data in terms of a quantum yield  
 391 because this normalizes for differences in light absorption by the sensitizers. Additionally,  
 392 calculating quantum yields for sensitizers also allows for the comparison to quantum yields  
 393 measured for the formation of hydroxylating species from DOM.

394 Second, there is the issue of the concentration of sensitizers changing with irradiation time.  
 395 To evaluate this second issue, solutions of only sensitizers were irradiated under the same  
 396 conditions described above and the absorbance spectra of those solutions were measured at  
 397 different irradiation times. Changes in concentration of sensitizers were observed for quinones  
 398 and hydroxybenzoic acids, which are the sensitizers that have been identified to have a  
 399 hydroxylating capacity, at both irradiation wavelengths (ESI Figures S5 and S6). Regarding  
 400 quinones, PBQ rapidly photodegrades under both wavelength conditions and A2S and DPBQ  
 401 undergo rapid photodegradation with 320 nm irradiation. For hydroxybenzoic acids, Figure S6  
 402 shows rapid photodegradation of DHBA at 320 nm. Quantum yields for these sensitizers at these  
 403 wavelengths were not calculated.

404 **Table 1.** Quantum yields estimates for the production of hydroxylating species using benzoic  
 405 acid and benzene as probe compound and irradiating at 254 and 320 nm, respectively. Values  
 406 represent average of at least triplicate measurements with error representing one standard  
 407 deviation. Values assume a  $Y_{\cdot\text{OH}}$  value of 0.63 and 0.15, equal to that of  $\cdot\text{OH}$ , for benzene and  
 408 benzoic acid, respectively. ND = No quantum yield data for sensitizer because direct  
 409 photodegradation of sensitizer occurred on a timescale too short for accurate quantum yield  
 410 computation. Direct photodegradation data can be found in the ESI, Figures S5 and S6.

Model Sensitizer	Benzoic Acid (254 nm irradiation) ( $\times 10^{-3}$ )	Benzene (320 nm irradiation) ( $\times 10^{-3}$ )
p-Benzoquinone (PBQ)	ND	ND
Anthraquinone-2-sulfonate (A2S)	$47 \pm 1.2$	ND

2,6-Dimethoxy-p-benzoquinone (DPBQ)	$17 \pm 0.55$	ND
2,4-Dihydroxybenzoic acid (DHBA)	$6.3 \pm 0.28$	ND
4-Hydroxybenzoic acid (4HBA)	$5.4 \pm 0.13$	$11 \pm 0.91$

411

412 Interestingly, although quinone degradation is significant, the formation rate of the

413 hydroxylated probe compounds remains constant over our experimental timeframe in all cases

414 but one (A2S), where it is expected that triplet A2S is reacting with phenol (Figures 3B). One

415 hypothesis is that the quinone and hydroxybenzoic acid photoproducts also have a hydroxylating

416 capacity. For quinones, this was tested by performing experiments with hydroquinone, a quinone

417 photoproduct,<sup>19</sup> using 320 nm lamps with benzene as the probe compound. The 320 nm lamps

418 emit at <300 nm, which overlaps with the absorption peak of hydroquinone (~290 nm). These

419 results can be found in the Figure S7. Production of phenol is observed in these experiments,

420 indicating that hydroquinone has a hydroxylating capacity, with an estimated formation rate of

421  $1.1 \times 10^{-9} \text{ M}^{-1} \text{ s}^{-1}$ , approximately an order of magnitude higher than the rate of formation of

422 phenol from the direct photolysis of benzene ( $1.94 \times 10^{-10} \text{ M}^{-1} \text{ s}^{-1}$ ). Based on these results, it is

423 hypothesized that the quantum yields for quinones presented in this study are representative of

424 the photochemistry of both quinones and quinone photoproducts, which could account for the

425 linear rate of formation despite the fast photodegradation of quinones in these experimental

426 conditions. The degradation of the hydroxybenzoic acids happens less rapidly than that of

427 quinones but is still not negligible, especially in the case of DHBA with 320 nm irradiation

428 (Figure S6). It is possible that the photoproducts of hydroxybenzoic acids also have a

429 hydroxylating capacity, but the photoproducts of these compounds are not well established

430 except for DHBA where a variety of carboxylated quinones and hydroxy-benzoic acids are

431 known to be formed and to have a hydroxylating capacity.<sup>63</sup> Based on the photochemical

432 behavior observed for hydroquinone, it is hypothesized that quantum yields presented in this

1  
2  
3 433 study are estimations for the quantum yields for the formation of hydroxylating species from a  
4  
5 434 combination of sensitizers and their photoproducts.  
6  
7

8 435 Quinone quantum yields at 254 nm for A2S and DPBQ were  $(47 \pm 1.2) \times 10^{-3}$  and  $(17 \pm$   
9  
10 436  $0.55) \times 10^{-3}$ , respectively. These values are approximately an order of magnitude lower than the  
11  
12 437 quantum yield value reported by Gan et al., which is  $0.37 \pm 0.04$ .<sup>19</sup> This difference may be due  
13  
14 438 the use of different probe compounds, benzoic acid used in this study and DMSO used by Gan et  
15  
16 439 al. Notably, a number have studies have concluded that DMSO is not a suitable probe for  
17  
18 440 detecting hydroxylating species produced from quinone photolysis.<sup>39; 40</sup> One study did not detect  
19  
20 441 a hydroxylating species from *p*-benzoquinone photolysis when using DMSO as a probe, while  
21  
22 442 another did but attributed this to the direct reaction of the triplet quinone with DMSO.<sup>39; 40</sup> Taken  
23  
24 443 as a whole, the existing data does not support the use of DMSO as a probe compound for the  
25  
26 444 production of hydroxylating species from quinone photolysis. Consequently, the quantum yield  
27  
28 445 measured by Gan et al. is questionable. Moreover, calculations performed to relate the  
29  
30 446 absorbance by quinones in DOM to the quantum yields measured in this study validate the order  
31  
32 447 of magnitude of the quantum yields presented here. For more information about these  
33  
34 448 calculations, see the Quinones and hydroxybenzoic acids contribution to DOM behavior section.  
35  
36  
37  
38  
39

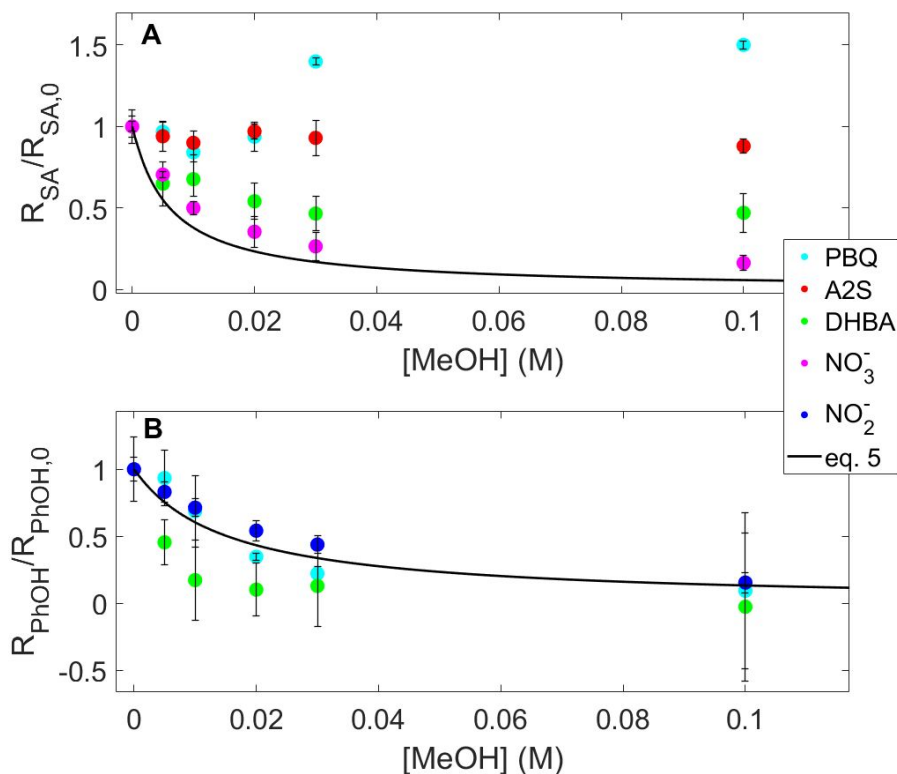
40 449 For hydroxybenzoic acids, variation in the quantum yields with wavelength was observed,  
41  
42 450  $(5.4 \pm 0.13) \times 10^{-3}$  at 254 nm and  $(11 \pm 0.91) \times 10^{-3}$  at 320 nm, for 4HBA (Table 1). There are  
43  
44 451 two possible reasons for variation in quantum yields: the wavelength dependence of the  
45  
46 452 photochemistry and the use of different probe compounds. In a study by Sun et al.,<sup>22</sup> variation in  
47  
48 453 quantum yield with wavelength was observed to range from  $(8.0 - 12.9) \times 10^{-3}$  over 290 - 320  
49  
50 454 nm for 2,4-dihydroxybenzoic acid and  $(10.0 - 11.3) \times 10^{-3}$  over 280 - 290 nm for 4-  
51  
52 455 hydroxybenzoic acid when using the same probe compound, indicating that the photochemical  
53  
54  
55  
56  
57  
58  
59  
60



1  
2  
3 456 pathway by which hydroxylating species are produced from this class of sensitizers is  
4  
5  
6 457 wavelength dependent. Additionally, the resulting quantum yield of  $(11 \pm 0.91) \times 10^{-3}$  for 4HBA  
7  
8 458 using the 320 nm lamps (wavelength range 270 to 400 nm) agrees well with the results published  
9  
10 459 by Sun et al.,  $(10.0 - 11.3) \times 10^{-3}$  over 280 – 290 nm, where benzene was also used as the probe  
11  
12 460 compound.<sup>22</sup>

### 15 461 *Methanol Quenching*

17 462 An important consideration to further understand the formation of hydroxylating species  
18  
19 463 from DOM is the ability to differentiate between  $\cdot\text{OH}$  and  $\cdot\text{OH}$ -like species. Methanol was used  
20  
21 464 as a quencher to investigate differences in the behavior of  $\cdot\text{OH}$  and other hydroxylating species  
22  
23 465 produced from quinones and hydroxybenzoic acids. These classes of sensitizers were selected  
24  
25 466 based on data in Figures 2 and 3, which established that both classes of sensitizers have a  
26  
27 467 hydroxylating capacity. Methanol reacts with  $\cdot\text{OH}$ , with a rate constant of  $9.7 \times 10^8 \text{ M}^{-1} \text{ s}^{-1}$ ,<sup>7</sup> but  
28  
29 468 the rate constant between methanol and other unknown hydroxylating species is unknown,  
30  
31 469 although it is hypothesized to be different. Methanol quenching was modeled using the rate  
32  
33 470 constant for  $\cdot\text{OH}$ , represented as the fraction of  $\cdot\text{OH}$  reacting with the probe compounds,  $f$ , as the  
34  
35 471 concentration of methanol increases, represented by eq. 5. Experimental data were compared to  
36  
37 472 the model,  $f$ , to assess similarities between the behavior of  $\cdot\text{OH}$  and other hydroxylating species.  
38  
39  
40  
41  
42  
43  
44  
45  
46  
47  
48  
49  
50  
51  
52  
53  
54  
55  
56  
57  
58  
59  
60



473

474 **Figure 4.** Effect of methanol addition ( $\cdot OH$  quencher) on the production of the hydroxylated  
 475 probe compound. Left axis, normalized experimental rates of formation for the photolysis of 20  
 476  $\mu M$  p-benzoquinone (PBQ), 20  $\mu M$  anthraquinone-2-sulfonate (A2S), 20  $\mu M$  2,4-  
 477 dihydroxybenzoic acid (DHBA), and 6 mM nitrate ( $NO_3^-$ ) with a probe compound in the  
 478 presence of 0, 0.005, 0.01, 0.02, 0.03, 0.1 M methanol. **A:** 1 mM benzoic acid as probe  
 479 compound, 254 nm lamps. **B:** 3 mM benzene as probe compound, 320 nm lamps.

480 Figure 4A shows normalized rates of hydroxylated probe compound formation for  
 481 experiments for different sensitizers using benzoic acid and 254 nm irradiation at different  
 482 methanol concentrations. Figure 4B shows the same plot but for 320 nm irradiation. Methanol  
 483 quenching of  $\cdot OH$  produced from the photolysis of nitrate and nitrite was measured to confirm  
 484 the modeled behavior of  $\cdot OH$ .<sup>64</sup> In experiments containing nitrate (Figure 4A) and nitrite (Figure  
 485 4B), there is good agreement between observed and calculated quenching (i.e.,  $f$  calculated via  
 486 eq. 5), especially considering the range of reported values for the rate constant of the reaction  
 487 between  $\cdot OH$  and methanol varies by about 20%.<sup>7</sup> Conversely, measured quenching for both

1  
2  
3 488 quinones and hydroxybenzoic acids exhibited stark and inconsistent differences with calculated  
4  
5 489 quenching in the two different probe/wavelength systems. For DHBA (a hydroxybenzoic acid  
6  
7 490 hypothesized to produce free  $\cdot\text{OH}$ ) with benzoic acid and 254 nm irradiation, there is incomplete  
8  
9 491 quenching of the production of salicylic acid with increasing concentrations of methanol (Figure  
10  
11 492 4A, green circles). Conversely, for this same sensitizer but using benzene with 320 nm  
12  
13 493 irradiation, methanol quenches the production of phenol to a greater degree than that modeled by  
14  
15 494  $\cdot\text{OH}$  (Figure 4B, green circles). Considering quinones, when using PBQ and A2S as the  
16  
17 495 sensitizers, no quenching of salicylic acid production by methanol was observed in samples  
18  
19 496 using benzoic acid with 254 nm irradiation. However, when using benzene with 320 nm  
20  
21 497 irradiation, PBQ exhibited quenching of the formation of phenol that was similar to that of  $\cdot\text{OH}$   
22  
23 498 (Figure 4B, cyan circles).

## 24 499 **DISCUSSION**

### 25 500 *Hydroxylating capacities of model sensitizers*

26 501 Data in Figures 2 and 3 are supportive of previous studies indicating that quinones and  
27  
28 502 hydroxybenzoic acids have a hydroxylating capacity. One previous study has reported the  
29  
30 503 detection of  $\cdot\text{OH}$  from the photolysis of hydroxybenzoic acids.<sup>22</sup> In this case, methane quenching  
31  
32 504 experiments were supportive that the hydroxylating species responsible was free  $\cdot\text{OH}$ . While  
33  
34 505 several mechanisms were postulated such as photoionization,<sup>22</sup> no definitive mechanism has  
35  
36 506 been established for the production of  $\cdot\text{OH}$  from hydroxybenzoic acids. The production of  
37  
38 507 hydroxylating species from quinones has been studied more extensively than that of  
39  
40 508 hydroxybenzoic acids. Studies have shown that the hydroxylating species produced by quinone  
41  
42 509 photolysis is not  $\cdot\text{OH}$ , but an  $\cdot\text{OH}$ -like species proposed to be a triplet quinone – water  
43  
44 510 exciplex.<sup>21</sup> Other studies suggest that if triplet quinones do form an exciplex with water, this

1  
2  
3 511 species proceeds directly to other photochemical degradation products of quinones, unless there  
4  
5 512 is sufficient concentration of other reactive compounds.<sup>19; 39; 42</sup> Additionally, previous work  
6  
7 513 indicated that the quantum yield for the formation of phenol from benzene in the presence of  
8  
9 514 PBQ had an activation energy near zero.<sup>20</sup> In this case, this behavior was attributed to a multi-  
10  
11 515 step process involving an exciplex.  
12  
13

14 516 Although data in Figures 3C and 3D could be taken as support that aromatic ketones and  
15  
16 517 other triplet forming species have a hydroxylating capacity, we hypothesize that this is not the  
17  
18 518 case for two reasons. First, to the best of our knowledge there is no known photochemistry for  
19  
20 519 aromatic ketones and the other triplet forming sensitizers that would lead to  $\cdot\text{OH}$  or other  
21  
22 520 hydroxylating species. Although prior studies have indicated that species having a very high  
23  
24 521 triplet state one electron reduction potential (e.g., A2S) are capable of oxidizing hydroxide to  
25  
26 522 form  $\cdot\text{OH}$ ,<sup>10; 23; 65</sup> the aromatic ketones and other triplet forming species in this study (Figure 1)  
27  
28 523 have lower one electron reduction potential than A2S. Second, these data are not in agreement  
29  
30 524 with the data from experiments using benzoic acid with 254 nm irradiation where salicylic acid  
31  
32 525 formation was attributed solely to the direct photolysis of benzoic acid. Because the rates of  
33  
34 526 formation for aromatic ketones and other triplet forming species are lower than that of the  
35  
36 527 quinones and hydroxybenzoic acids (Table S3) and the formation is thought to be dependent on  
37  
38 528 the probe compound and irradiation wavelength, for the purposes of this study, they are not be  
39  
40 529 considered significant contributors to the overall production of hydroxylating species from  
41  
42 530 DOM. Overall, the data displayed in Figures 2 and 3 is consistent with previous publications,  
43  
44 531 confirming the presence of hydroxylating species from the photolysis of quinones and  
45  
46 532 hydroxybenzoic acids.<sup>19-22; 35; 42</sup>  
47  
48  
49  
50  
51  
52

53  
54 533 ***Methanol quenching: Hydroxybenzoic acids***  
55  
56  
57  
58  
59  
60

1  
2  
3 534 There are a few possible explanations for behavior observed in the DHBA methanol  
4  
5 535 quenching data (Figure 4). One is that the hydroxylating species produced from the photolysis of  
6  
7 536 DHBA is not  $\cdot\text{OH}$  (in contrast with a study by Sun et al.)<sup>22</sup> and this  $\cdot\text{OH}$ -like species has rate  
8  
9  
10 537 constants with benzene, benzoic acid, and methanol that are different than  $\cdot\text{OH}$ , resulting in a  
11  
12 538 trend in the methanol quenching data that differs from that of  $\cdot\text{OH}$ . Interestingly, if this  $\cdot\text{OH}$ -like  
13  
14 539 species has a rate constant with benzene that is an order of magnitude lower than that of  $\cdot\text{OH}$ ,  
15  
16 540  $7.80 \times 10^8 \text{ M}^{-1} \text{ s}^{-1}$  instead of  $7.80 \times 10^9 \text{ M}^{-1} \text{ s}^{-1}$ , then the experimental behavior of this  
17  
18  
19 541 hydroxylating species in the presence of benzene and methanol would match the model  
20  
21 542 represented by eq. 5 which is shown in Figure S8 in the ESI. However, not only is this  
22  
23 543 hypothesis at odds with more stringent methane quenching data reported by Sun et al.<sup>22</sup> that  
24  
25 544 indicated that the photolysis of hydroxybenzoic acids produces free  $\cdot\text{OH}$ , but it also only explains  
26  
27 545 the behavior of DHBA in systems using benzene with 320 nm irradiation, not for benzoic acid  
28  
29 546 with 254 nm irradiation. Sun et al.<sup>22</sup> used different quenchers and probe compound to determine  
30  
31 547 whether the hydroxylating species detected was free  $\cdot\text{OH}$  than those that were used in our study,  
32  
33 548 including methane as a probe compound selective for  $\cdot\text{OH}$  and formate as a competitor with  
34  
35 549 benzene, which could be responsible for the conflicting results.<sup>22</sup>  
36  
37  
38  
39

40 550 Another possible explanation for the behavior in systems containing DHBA is that there  
41  
42 551 are other photochemical pathways contributing to the formation and quenching of salicylic acid  
43  
44 552 and phenol. One possible pathway that was tested, relevant to the use of benzoic acid with 254  
45  
46 553 nm irradiation, is production of salicylic acid from the direct photolysis of DHBA (Figure S3). If  
47  
48 554 salicylic acid was being produced from the direct photolysis of DHBA as well as the reaction of  
49  
50 555 the hydroxylating intermediate, that could explain the incomplete quenching of the formation of  
51  
52 556 salicylic acid by methanol. However, no formation of salicylic acid was observed from the direct  
53  
54  
55  
56  
57  
58  
59  
60

1  
2  
3 557 photolysis of DHBA (Figure S3), so the incomplete quenching of salicylic acid from the  
4  
5 558 photolysis of DHBA is unaccounted for. Overall, the conflicting results described in Figure 4  
6  
7  
8 559 demonstrate that methanol cannot distinguish between  $\cdot\text{OH}$  and  $\cdot\text{OH}$ -like species from  
9  
10 560 hydroxybenzoic acids.

### 11 12 561 *Methanol quenching: Quinones*

13  
14 562 Quinones (PBQ and A2S) exhibited no quenching of salicylic acid formation in  
15  
16  
17 563 experiments using benzoic acid with 254 nm irradiation upon methanol addition. Conversely,  
18  
19 564 when using benzene with 320 nm irradiation, the quenching of phenol formation from quinone  
20  
21 565 photolysis was similar to quenching observed for known free  $\cdot\text{OH}$  sources (Figure 4). There are a  
22  
23  
24 566 few possible explanations for this behavior. One hypothesis for the difference in the 254 nm and  
25  
26 567 320 nm quenching data for quinones is that there are different hydroxylating intermediates being  
27  
28 568 produced at the two wavelengths, one of which does not react with methanol, resulting in the  
29  
30  
31 569 absence of quenching behavior. It is possible that at 254 nm the hydroxylating species produced  
32  
33 570 from quinone photolysis is the  $\cdot\text{OH}$ -like species and that this species is not quenched by  
34  
35 571 methanol and that at 320 nm  $\cdot\text{OH}$  is produced, which has a well-known rate constant with  
36  
37  
38 572 methanol.<sup>7</sup> One study that utilized electron paramagnetic resonance (EPR) to investigate the  
39  
40 573 reactivity of t-butanol with  $\cdot\text{OH}$  produced from  $\text{H}_2\text{O}_2$  and from PBQ photolysis observed that t-  
41  
42 574 butanol was much more effective at reacting with  $\cdot\text{OH}$  produced from  $\text{H}_2\text{O}_2$  than  $\cdot\text{OH}$  produced  
43  
44 575 from PBQ photolysis, leading to the conclusion that the hydroxylating species observed in the  
45  
46  
47 576 EPR spectra is not  $\cdot\text{OH}$ .<sup>39</sup> This study supports the hypothesis that alcohols react more slowly  
48  
49 577 with  $\cdot\text{OH}$ -like species than with  $\cdot\text{OH}$  and that differences in the methanol quenching data shown  
50  
51 578 in this study could be attributed to the presence of different hydroxylating species at the two  
52  
53  
54 579 wavelengths tested.

1  
2  
3 580 The second hypothesis is that the lack of quenching in the system using benzoic acid with  
4  
5 581 254 nm irradiation is due to the formation of salicylic acid from one-electron oxidation of  
6  
7 582 benzoic acid by the triplet quinone, with the sum of the production from the hydroxylating  
8  
9 583 species and the one-electron oxidation of benzoic acid by the triplet quinone. However, the  
10  
11 584 oxidation potential of benzoic acid calculated using the formula found in Jonsson et al.<sup>62</sup> is 2.56  
12  
13 585 V (with an associated error that can be estimated to be  $\pm 0.2$ V) and the reduction potential of  
14  
15 586 triplet PBQ is 2.42 V,<sup>10</sup> so if this reaction does happen it is anticipated to occur slowly. If the  
16  
17 587 formation of salicylic acid in these experimental conditions is mostly due to the reaction of  
18  
19 588 triplet quinones with benzoic acid, it is expected that there would still be only limited decrease in  
20  
21 589 the quenching trend in Figure 4. The decrease would be due to the quenching of hydroxylating  
22  
23 590 species by methanol and to an eventual reaction of the triplet quinone with methanol.

24  
25  
26 591 It is important to note that studies have shown that the photoreduction of triplet quinones  
27  
28 592 happens in the presence of hydrogen donors, such as alcohols.<sup>39</sup> The reaction between triplet  
29  
30 593 quinones and methanol is thought to produce a carbon centered radical, which can then react  
31  
32 594 with ground state quinone to form formaldehyde.<sup>39</sup> The formation of formaldehyde was not  
33  
34 595 measured in this study. To assess the contribution of methanol to reaction pathways of triplet  
35  
36 596 quinone a calculation for the fraction of triplet quinone reacting with methanol in a system  
37  
38 597 containing water, benzoic acid, methanol, and oxygen was performed using eq. 6 and a figure  
39  
40 598 displaying this data is presented in the ESI, Figure S9, using the following rate constants. The  
41  
42 599 rate constant for the reaction of triplet *p*-benzoquinone and oxygen is reported to be  $2 \times 10^9$  M<sup>-1</sup>  
43  
44 600 s<sup>-1</sup> and the rate constant for the reaction between triplet *p*-benzoquinone and methanol is reported  
45  
46 601 to be  $4.2 \times 10^7$  M<sup>-1</sup> s<sup>-1</sup>.<sup>39</sup> The rate constant of triplet methyl-*p*-benzoquinone with water has been  
47  
48 602 estimated to be  $7.3 \times 10^4$  M<sup>-1</sup> s<sup>-1</sup>.<sup>19</sup> The rate constant for the reaction between benzoic acid and  
49  
50  
51  
52  
53  
54  
55  
56  
57  
58  
59  
60

triplet quinones has not been quantified. For this reason, eq. 6 was calculated using values for  $k_{BA}$  ranging from  $10^4 - 10^9 \text{ M}^{-1} \text{ s}^{-1}$  to assess the potential effect of this reaction.

$$f_{MeOH} = \frac{k_{MeOH}[MeOH]}{k_{MeOH}[MeOH] + k_{BA}[BA] + k_{H_2O}[H_2O] + k_{O_2}[O_2]} \quad (6)$$

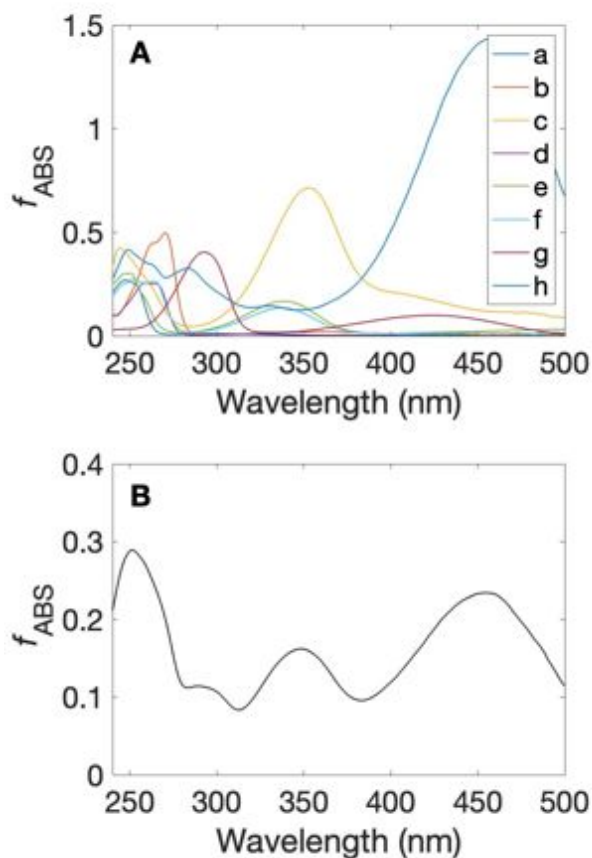
According to Figure S9, at methanol concentrations lower than 0.03 M approximately 20% or less of triplet quinone reacts with methanol. At the highest concentration of methanol, 0.1 M, no more than 50% of the triplet quinone reacts with methanol, depending on the rate constant for the reaction of benzoic acid and the triplet quinone. It is possible that complex chemistry involving methanol reactivity with triplet quinones in the presence of benzoic acid is contributing to a fraction of the lack of quenching observed in Figure 4A. Ultimately, the conflicting quenching trends for quinones, the use of different probes at the two wavelengths used in this study, and the possibility of the reaction of methanol with triplet quinones leave the question of the chemistry of the hydroxylating intermediate produced from quinone photolysis in question.

### ***Quinones and hydroxybenzoic acids contribution to DOM behavior***

To assess the role of quinones as sensitizers for production of  $\cdot\text{OH}$  and  $\cdot\text{OH}$ -like species, the contribution of quinones and hydroxybenzoic acids to the fraction of light absorbed by DOM was calculated, using electrochemical data for Suwannee River fulvic acid (SRFA)<sup>66</sup> Similar calculations were done in a study by Ma et al.<sup>67</sup> Electron accepting capacities (EAC,  $\mu\text{mol}_{e^-} \text{ g}_{\text{HS}^{-1}}$ ) were used to calculate the concentration of quinones ( $\text{EAC} \times \mu\text{mol}_{\text{quinone}}/2 \mu\text{mol}_{e^-}$ ) and electron donating capacities (EDC,  $\mu\text{mol}_{e^-} \text{ g}_{\text{HS}^{-1}}$ ) were used to calculate the concentration of hydroxybenzoic acids ( $\text{EDC} \times \mu\text{mol}_{\text{hydroxybenzoic acid}}/2 \mu\text{mol}_{e^-}$ ). EDC and EAC measurements are dependent on solutions conditions, which might not be identical to solution conditions of DOM photochemistry experiments. The absorbance due to quinones and hydroxybenzoic acids was



1  
2  
3 625 calculated by multiplying the above calculated concentrations by the molar absorption  
4  
5 626 coefficient for these compounds measured in our study. The results of these calculations are  
6  
7 627 shown in Figure 5 and in Table S4 (for detailed calculations, see Text S3, ESI). For the  
8  
9 628 hydroxybenzoic acid sensitizers, 4HBA and DHBA, the fraction of light absorbed at 300 nm  
10  
11 629 ranged from 0.2% by 4HBA to 47.9% by DHBA, whereas at 254 nm the fraction of light  
12  
13 630 absorbed by 4HBA is 86.0% and the fraction of light absorbed by DHBA is 47.9%. Figure 5A  
14  
15 631 shows that the fraction of light absorbed by quinones depends on the specific compound and  
16  
17 632 wavelength. As a surrogate for the variety of quinone structures in a given DOM sample eight  
18  
19 633 quinones were used to approximate the total quinone absorbance, shown in Figure 5B. In this  
20  
21 634 approximation (Figure 5B) quinone absorbance falls in the 1.5 – 22% range. For two quinone  
22  
23 635 sensitizers in this study (PBQ and DPBQ), values ranged between nearly 31% (by PBQ at 246  
24  
25 636 nm) and <1% (by PBQ at 424 nm). For quinones whose absorption spectrum extends into the far  
26  
27 637 UV and visible, the fraction of light absorbed at longer wavelengths increases (e.g., 15.2 % by  
28  
29 638 1,4-naphthoquinone at 342 nm). For DPBQ, the product of the observed quantum yield at 254 nm  
30  
31 639 as an estimate for the quinone quantum yield ( $17 \times 10^{-3}$ , Table 1) and the fraction of light  
32  
33 640 absorbed by the mixture of quinones at within the range of wavelengths shown in Figure 5B (1.5  
34  
35 641 – 22%), at 254 nm the quantum yield would be  $\sim 4.8 \times 10^{-3}$ . A study by Lester et al. showed that  
36  
37 642 quantum yields for the formation of hydroxylating species from DOM photolysis at 254 nm is  
38  
39 643 generally an order of magnitude higher than the quantum yield values at wavelengths greater  
40  
41 644 than 300 nm, with the quantum yield for the formation of hydroxylating species from SRFA  
42  
43  
44  
45  
46  
47  
48  
49 645 being 0.047.<sup>68</sup>



646  
 647 **Figure 5.** Fraction of light absorbed ( $f_{ABS}$ ) by quinones in DOM. **A:** Fraction of light absorbance  
 648 by a: p-benzoquinone, b: 2,3,5,6-tetramethyl-1,4-benzoquinone, c: 2,5-diphenyl-1,4-  
 649 benzoquinone, d: 2,5-di-tert-butyl-1,4-benzoquinone, e: 1,4-naphthoquinone, f: 2-methyl-1,4-  
 650 naphthoquinone, g: 2,6-dimethoxy-p-benzoquinone, and h: alizarin, calculated individually, as  
 651 though each account for entirety of quinone content in SRFA. **B:** Fraction of absorbance by  
 652 quinones a – h from above to account for quinone content of DOM in equal parts (12.5% each).  
 653

654 A recent study by Leresche et al. measuring the hydroxylating capacity of DOM before  
 655 and after ozonation attributed the increase in quantum yields for hydroxylating species to the  
 656 increase in quinone content of DOM post-oxidation.<sup>48</sup> Our results support the hypothesis that  
 657  $^3\text{DOM}^*$ , including quinones, are precursors of  $\cdot\text{OH}$  and  $\cdot\text{OH}$ -like species from DOM photolysis.  
 658 However, another recent study suggested that  $^3\text{DOM}^*$  is not a major precursor to  $\cdot\text{OH}$  or  $\cdot\text{OH}$ -  
 659 like species based on correlations between RI quantum yields and the abundance of various  
 660 formulas from ultra-high-resolution mass spectrometry.<sup>69</sup> Instead, it was suggested that  $^1\text{DOM}^*$ ,

1  
2  
3 661 charge-transfer states, or exciplexes involving photochemically excited DOM may be involved.<sup>69</sup>  
4  
5 662 This hypothesis is consistent with the role of hydroxybenzoic acids as sensitizers, but not with  
6  
7 663 quinones. We contend that triplet quinones are likely responsible for some of the hydroxylation  
8  
9 664 reactions observed for aromatic probe compounds given the known presence of these moieties in  
10  
11 665 DOM. Additionally, our study demonstrates quinones do not necessarily need to be photostable  
12  
13 666 in order to contribute significantly to the  $\cdot\text{OH}$  or  $\cdot\text{OH}$ -like production. For example, we observed  
14  
15 667 similar rates of hydroxylation reactions from hydroquinone, a phenol photoproduct.  
16  
17  
18  
19 668

## 20 21 669 **CONCLUSION**

22  
23  
24 670 The goal of this work was to further understand the formation of  $\cdot\text{OH}$  and  $\cdot\text{OH}$ -like  
25  
26 671 species from DOM photolysis. These results build on prior work that has established that  
27  
28 672 quinones and hydroxybenzoic acids have a hydroxylating capacity.<sup>19; 21; 22; 34; 39; 42</sup> Aromatic  
29  
30 673 ketones and other triplet forming species were selected to account for a class of sensitizers that  
31  
32 674 are responsible for a portion of reactive triplet species in DOM. Aromatic ketones and other  
33  
34 675 triplet forming species were expected to be negative controls for the production of hydroxylating  
35  
36 676 intermediates.  
37  
38  
39

40 677 The results presented in this study have several implications for measurement of  
41  
42 678 hydroxylating species formation from DOM photolysis. Testing both benzoic acid and benzene  
43  
44 679 as probe compound shed light on their respective effectiveness as probe compound for hydroxyl  
45  
46 680 radicals and, more generally, hydroxylating species. Additionally, the quenching of phenol  
47  
48 681 formation from benzene during quinone photolysis by methanol indicates that methanol reacts  
49  
50 682 with both  $\cdot\text{OH}$  and  $\cdot\text{OH}$ -like species. Although this result has been demonstrated in the literature,  
51  
52  
53  
54  
55  
56  
57  
58  
59  
60

1  
2  
3 683 methanol has not been used explicitly to assess the reactivity of  $\cdot\text{OH}$ -like species derived from  
4  
5 684 triplet quinones.

6  
7  
8 685 The probes molecules used in this study are often used to estimate  $\cdot\text{OH}$  steady-state  
9  
10 686 concentration ( $[\cdot\text{OH}]_{\text{ss}}$ ) in surface waters without distinguishing between  $\cdot\text{OH}$  and other  
11  
12 687 hydroxylating species, leading to a potential over estimation of  $[\cdot\text{OH}]_{\text{ss}}$ . This can potentially lead  
13  
14 688 to an erroneous estimation of the  $\cdot\text{OH}$  influence on the fate of micropollutants, e.g., if one uses  
15  
16 689 an over evaluated  $[\cdot\text{OH}]_{\text{ss}}$  and the second-order rate constant between  $\cdot\text{OH}$  and the micropollutant  
17  
18 690 to evaluate the rate of transformation of a micropollutant due to  $\cdot\text{OH}$ .

19  
20  
21 691 Taken as a whole, the results of this study provide further support for the role of quinones  
22  
23 692 and hydroxybenzoic acids as sensitizers for the production hydroxylating species from DOM  
24  
25 693 photolysis. An important finding is that photoproducts from these species, especially in the case  
26  
27 694 of quinones, likely have a hydroxylating capacity as well. Methanol quenching as a test of  
28  
29 695 hydroxylating species' identity was inconclusive, indicating that other quenchers are needed to  
30  
31 696 assess these differences in reactivity. Additionally, the quantum yields of  $\cdot\text{OH}$  and  $\cdot\text{OH}$ -like  
32  
33 697 species from sensitizers photolysis are comparable to values measured for DOM by taking into  
34  
35 698 account the fraction of light absorbed by quinones within DOM. These results indicate that  
36  
37 699 triplet state quinones play a role in the hydroxylating capacity of DOM.

40  
41  
42 700

## 43 44 701 **Acknowledgements**

45  
46  
47  
48 702 Funding for this study came from the US National Science Foundation (CBET #1453906  
49  
50  
51  
52 703 and CHE #1808126) and through the University of Colorado Discovery Learning  
53  
54  
55 704 Apprenticeship.

1  
2  
3 705 **Associated Content**  
4  
5

6  
7 706 **Electronic Supplementary Information (ESI)**  
8  
9

10 707 The electronic supplementary information is available at DOI:  
11  
12

13  
14 708  
15

16  
17 709 **Author information**  
18  
19

20  
21 710 Corresponding authors  
22  
23

24 711 \*E-mail: gmckay@tamu.edu; Fernando.rosario@colorado.edu  
25

26 712 **ORCID**  
27

28 713 Kylie Couch: 0000-0003-3392-6830  
29

30  
31 714 Frank Leresche: 0000-0001-8400-3142  
32

33 715 Claire Farmer: 0000-0002-8341-2144  
34

35 716 Garrett McKay: 0000-0002-6529-0892  
36

37  
38 717 Fernando Rosario-Ortiz: 0000-0002-3311-9089  
39

40 718 **Note**  
41  
42

43 719 The authors declare no competing financial interest.  
44  
45

46  
47 720  
48  
49  
50  
51  
52  
53  
54  
55  
56  
57  
58  
59  
60

721 **References**

- 722 1. Southworth BA, Voelker BM. Hydroxyl radical production via the photo-fenton reaction in  
723 the presence of fulvic acid. *Environ. Sci. Technol.*, 2003, 37(6):1130-1136.
- 724 2. Vaughan PP, Blough NV. Photochemical formation of hydroxyl radical by constituents of  
725 natural waters. *Environ. Sci. Technol.*, 1998, 32(19):2947-2953.
- 726 3. Vione D, Falletti G, Maurino V, Minero C, Pelizzetti E, Malandrino M, Ajassa R, Olariu RI,  
727 Arsene C. 2006. Sources and sinks of hydroxyl radicals upon irradiation of natural water  
728 samples. *Environ. Sci. Technol.*, 2006, 40(12):3775-3781.
- 729 4. Wenk J, von Gunten U, Canonica S. Effect of dissolved organic matter on the transformation  
730 of contaminants induced by excited triplet states and the hydroxyl radical. *Environ. Sci. Technol.*,  
731 2011, 45(4):1334-1340.
- 732 5. Xu HM, Cooper WJ, Jung J, Song WH. Photosensitized degradation of amoxicillin in natural  
733 organic matter isolate solutions. *Water Res.*, 2011, 45(2):632-638.
- 734 6. Boreen AL, Arnold WA, McNeill K. Photodegradation of pharmaceuticals in the aquatic  
735 environment: A review. *Aquat. Sci.*, 2003, 65(4):320-341.
- 736 7. Buxton GV, Greenstock CL, Helman WP, Ross AB. Critical-review of rate constants for  
737 reactions of hydrated electrons, hydrogen-atoms and hydroxyl radicals ( $\bullet\text{OH}/\bullet\text{O}^-$ ) in aqueous-  
738 solution. *J. Phys. Chem. Ref. Data*, 1988, 17(2):513-886.
- 739 8. Latch DE, Stender BL, Packer JL, Arnold WA, McNeill K. Photochemical fate of  
740 pharmaceuticals in the environment: Cimetidine and ranitidine. *Environ. Sci. Technol.*, 2003,  
741 37(15):3342-3350.
- 742 9. McConville MB, Mezyk SP, Remucal CK. Indirect photodegradation of the lampricides TFM  
743 and niclosamide. *Environ. Sci.: Processes Impacts*, 2017, 19(8):1028-1039.
- 744 10. McNeill K, Canonica S. Triplet state dissolved organic matter in aquatic photochemistry:  
745 Reaction mechanisms, substrate scope, and photophysical properties. *Environ. Sci.: Processes*  
746 *Impacts*, 2016, 18(11):1381-99.
- 747 11. Packer JL, Werner JJ, Latch DE, McNeill K, Arnold WA. Photochemical fate of  
748 pharmaceuticals in the environment: Naproxen, diclofenac, clofibric acid, and ibuprofen. *Aquat.*  
749 *Sci.*, 2003, 65(4):342-351.
- 750 12. Scully FE, Hoigné J. Rate constants for reactions of singlet oxygen with phenols and other  
751 compounds in water. *Chemosphere*, 1987, 16(4):681-694.
- 752 13. Rosario-Ortiz FL, Canonica S. Probe compounds to assess the photochemical activity of  
753 dissolved organic matter. *Environ. Sci. Technol.*, 2016, 50(23):12532-12547.
- 754 14. Vione D, Minella M, Maurino V, Minero C. Indirect photochemistry in sunlit surface waters:  
755 Photoinduced production of reactive transient species. *Chemistry*, 2014, 20(34):10590-10606.
- 756 15. Miller CJ, Rose AL, Waite TD. Hydroxyl radical production by  $\text{H}_2\text{O}_2$ -mediated oxidation of  
757  $\text{Fe}(\text{II})$  complexed by suwannee river fulvic acid under circumneutral freshwater conditions.  
758 *Environ. Sci. Technol.*, 2013, 47(2):829-835.
- 759 16. White EM, Vaughan PP, Zepp RG. Role of the photo-fenton reaction in the production of  
760 hydroxyl radicals and photobleaching of colored dissolved organic matter in a coastal river of the  
761 southeastern united states. *Aquat. Sci.*, 2003, 65(4):402-414.
- 762 17. Mopper K, Zhou XL. Hydroxyl radical photoproduction in the sea and its potential impact on  
763 marine processes. *Science*, 1990, 250(4981):661-664.

- 1  
2  
3 764 18. Page SE, Arnold WA, McNeill K. Assessing the contribution of free hydroxyl radical in  
4 765 organic matter-sensitized photohydroxylation reactions. *Environ. Sci. Technol.*, 2011,  
5 766 45(7):2818-2825.
- 6 767 19. Gan D, Jia M, Vaughan PP, Falvey DE, Blough NV. Aqueous photochemistry of methyl-  
7 768 benzoquinone. *J. Phys. Chem. A*, 2008, 112(13):2803-2812.
- 8 769 20. McKay G, Rosario-Ortiz FL. Temperature dependence of the photochemical formation of  
9 770 hydroxyl radical from dissolved organic matter. *Environ. Sci. Technol.*, 2015, 7;49(7):4147-54.
- 10 771 21. Pochon A, Vaughan PP, Gan DQ, Vath P, Blough NV, Falvey DE. Photochemical oxidation  
11 772 of water by 2-methyl-1,4-benzoquinone: Evidence against the formation of free hydroxyl radical.  
12 773 *J. Phys. Chem. A*, 2002, 106(12):2889-2894.
- 13 774 22. Sun LN, Qian JG, Blough NV, Mopper K. Insights into the photoproduction sites of hydroxyl  
14 775 radicals by dissolved organic matter in natural waters. *Environ. Sci. Technol. Lett.*, 2015,  
15 776 2(12):352-356.
- 16 777 23. Vione D, Ponzio M, Bagnus D, Maurino V, Minero C, Carlotti ME. Comparison of different  
17 778 probe molecules for the quantification of hydroxyl radicals in aqueous solution. *Environ. Chem.*  
18 779 *Lett.*, 2010, 8(1):95-100.
- 19 780 24. Zepp RG, Baughman GL, Schlotzhauer PF. Comparison of photochemical behavior of  
20 781 various humic substances in water: II. Photosensitized oxygenations. *Chemosphere*, 1981,  
21 782 10:119-126.
- 22 783 25. Canonica S, Jans U, Stemmler K, Hoigné J. Transformation kinetics of phenols in water:  
23 784 Photosensitization by dissolved natural organic material and aromatic ketones. *Environ. Sci.*  
24 785 *Technol.*, 1995, 29(7):1822-1831.
- 25 786 26. McKay G. Emerging investigator series: Critical review of photophysical models for the  
26 787 optical and photochemical properties of dissolved organic matter. *Environ. Sci.: Processes*  
27 788 *Impacts*, 2020, 22(5):1139-1165.
- 28 789 27. Sharpless CM, Blough NV. The importance of charge-transfer interactions in determining  
29 790 chromophoric dissolved organic matter (CDOM) optical and photochemical properties. *Environ.*  
30 791 *Sci.: Processes Impacts*, 2014, 16(4):654-671.
- 31 792 28. Vialykh EA, McKay G, Rosario-Ortiz FL. Computational assessment of the three-  
32 793 dimensional configuration of dissolved organic matter chromophores and influence on  
33 794 absorption spectra. *Environ. Sci. Technol.*, 2020, 54(24):15904-15913.
- 34 795 29. McKay G, Korak JA, Erickson PR, Latch DE, McNeill K, Rosario-Ortiz FL. The case  
35 796 against charge transfer interactions in dissolved organic matter photophysics. *Environ. Sci.*  
36 797 *Technol.*, 2018, 52(2):406-414.
- 37 798 30. Burns JM, Cooper WJ, Ferry JL, King DW, DiMento BP, McNeill K, Miller CJ, Miller WL,  
38 799 Peake BM, Rusak SA et al. Methods for reactive oxygen species (ROS) detection in aqueous  
39 800 environments. *Aquat. Sci.*, 2012, 74(4):683-734.
- 40 801 31. Dong MM, Rosario-Ortiz FL. Photochemical formation of hydroxyl radical from effluent  
41 802 organic matter. *Environ. Sci. Technol.*, 2012, 46(7):3788-3794.
- 42 803 32. Ononye AI, McIntosh AR, Bolton JR. Mechanisms of the photochemistry of p-benzoquinone  
43 804 in aqueous solutions. 1. Spin trapping and flash photolysis electron paramagnetic resonance  
44 805 studies. *J. Phys. Chem.*, 1986, 90(23):6266-6270.
- 45 806 33. Page SE, Arnold WA, McNeill K. Terephthalate as a probe for photochemically generated  
46 807 hydroxyl radical. *J. Environ. Monit.*, 2010, 12(9):1658-1665.
- 47 808 34. Alegria AE, Ferrer A, Sepulveda E. Photochemistry of water-soluble quinones. Production of  
48 809 a water-derived spin adduct. *Photochem. Photobiol.*, 1997, 66(4):436-442.
- 49  
50  
51  
52  
53  
54  
55  
56  
57  
58  
59  
60

- 1  
2  
3 810 35. Alegria AE, Ferrer A, Santiago G, Sepulveda E, Flores W. Photochemistry of water-soluble  
4 811 quinones. Production of the hydroxyl radical, singlet oxygen and the superoxide ion. *Photochem.*  
5 812 *Photobiol., A Chem.*, 1999, 127(1-3):57-65.  
6  
7 813 36. Ononye AI, Bolton JR. Mechanism of the photochemistry of p-benzoquinone in aqueous-  
8 814 solutions. 2. Optical flash-photolysis studies. *J. Phys. Chem.*, 1986 90(23):6270-6274.  
9 815 37. Pou S, Hassett DJ, Britigan BE, Cohen MS, Rosen GM. Problems associated with spin  
10 816 trapping oxygen-centered free-radicals in biological-systems. *Anal. Biochem.*, 1989 177(1):1-6.  
11 817 38. Ebersson L, Persson O. Generation of acyloxyl spin adducts from N-tert-butyl- $\alpha$ -  
12 818 phenylnitron (PBM) and 4,5-dihydro-5,5-dimethylpyrrole 1-oxide (DMPO) via  
13 819 nonconventional mechanisms. *J. Chem. Soc., Perkin Trans.*, 1997, 2, (9):1689-1696.  
14 820 39. von Sonntag J, Mvula E, Hildenbrand K, von Sonntag C. Photohydroxylation of 1,4-  
15 821 benzoquinone in aqueous solution revisited. *Chem. Eur. J.*, 2004, 10(2):440-451.  
16 822 40. Gorner H. Photoreactions of p-quinones with dimethyl sulfide and dimethyl sulfoxide in  
17 823 aqueous acetonitrile. *Photochem. Photobiol.*, 2006, 82(1):71-77.  
18 824 41. Beck SM, Brus LE. Photo-oxidation of water by para-benzoquinone. *J. Am. Chem. Soc.*,  
19 825 1982, 104(4):1103-1104.  
20 826 42. Gorner H. Photoprocesses of p-benzoquinones in aqueous solution. *J. Phys. Chem. A*, 2003,  
21 827 107(51):11587-11595.  
22 828 43. Sun LN, Chen HM, Abdulla HA, Mopper K. Estimating hydroxyl radical photochemical  
23 829 formation rates in natural waters during long-term laboratory irradiation experiments. *Environ.*  
24 830 *Sci.: Processes Impacts*, 2014, 16(4):757-763.  
25 831 44. Loeff I, Treinin A, Linschitz H. Photochemistry of 9,10-anthraquinone-2-sulfonate in  
26 832 solution. 1. Intermediates and mechanism. *J. Phys. Chem.*, 1983, 87(14):2536-2544.  
27 833 45. Jin S, Mofidi AA, Linden KG. Polychromatic UV fluence measurement using chemical  
28 834 actinometry, biosimetry, and mathematical techniques. *J. Environ. Engin.*, 2006, 132(8):831-  
29 835 841.  
30 836 46. Laszakovits JR, Berg SM, Anderson BG, O'Brien JE, Wammer KH, Sharpless CM. P-  
31 837 nitroanisole/pyridine and p-nitroacetophenone/pyridine actinometers revisited: Quantum yield in  
32 838 comparison to ferrioxalate. *Environ. Sci. Technol. Lett.*, 2017, 4(1):11-14.  
33 839 47. Zhou XL, Mopper K. Determination of photochemically produced hydroxyl radicals in  
34 840 seawater and freshwater. *Mar. Chem.*, 1990, 30(1-3):71-88.  
35 841 48. Leresche F, Torres-Ruiz JA, Kurtz T, von Gunten U, Rosario-Ortiz FL. Optical properties  
36 842 and photochemical production of hydroxyl radical and singlet oxygen after ozonation of  
37 843 dissolved organic matter. *Environ. Sci.: Water Res. Technol.*, 2021, 7(2):346-356.  
38 844 49. Garg S, Rose AL, Waite TD. Photochemical production of superoxide and hydrogen  
39 845 peroxide from natural organic matter. *Geochim. Cosmochim. Acta*, 2011, 75(15):4310-4320.  
40 846 50. Garg S, Rose AL, Waite TD. Production of reactive oxygen species on photolysis of dilute  
41 847 aqueous quinone solutions. *Photochem. Photobiol.*, 2007, 83(4):904-913.  
42 848 51. Goldstein S, Aschengrau D, Diamant Y, Rabani J. Photolysis of aqueous H<sub>2</sub>O<sub>2</sub>: Quantum  
43 849 yield and applications for polychromatic UV actinometry in photoreactors. *Environ. Sci.*  
44 850 *Technol.*, 2007, 41(21):7486-7490.  
45 851 52. Rabani J, Klugroth D, Henglein A. Pulse radiolytic investigations of OHCH<sub>2</sub>O<sub>2</sub> radicals. *J.*  
46 852 *Phys. Chem.*, 1974, 78(21):2089-2093.  
47 853 53. Arakaki T, Faust BC. Sources, sinks, and mechanisms of hydroxyl radical  $\cdot$ OH  
48 854 photoproduction and consumption in authentic acidic continental cloud waters from Whiteface  
49  
50  
51  
52  
53  
54  
55  
56  
57  
58  
59  
60



- 1  
2  
3 855 Mountain, New York: The role of the Fe(II, III) photochemical cycle. *J. Geophys. Res.*  
4 856 *Atmos.*, 1998, 103(D3):3487-3504.
- 5 857 54. Balakrishnan I, Reddy MP. Effect of temperature on gamma-radiolysis of aqueous-solutions.  
6 858 *J. Phys. Chem.*, 1972, 76(9):1273-1279.
- 7 859 55. Charbouillot T, Brigante M, Mailhot G, Maddigapu PR, Minero C, Vione D. Performance  
8 860 and selectivity of the terephthalic acid probe for  $\cdot\text{OH}$  as a function of temperature, pH and  
9 861 composition of atmospherically relevant aqueous media. *Photochem. Photobiol. A Chem.*, 2011,  
10 862 222(1):70-76.
- 11 863 56. Deister U, Warneck P, Wurzinger C. OH radicals generated by  $\text{NO}_3^-$  photolysis in aqueous-  
12 864 solution: competition kinetics and a study of the reaction  $\text{OH} + \text{CH}_2(\text{OH})\text{SO}_3^-$ . *Ber. Bunsen-*  
13 865 *Gesell. Phys. Chem.*, 1990, 94(5):594-599.
- 14 866 57. Van Buren J, Prasse C, Marron EL, Skeel B, Sedlak DL. Ring-cleavage products produced  
15 867 during the initial phase of oxidative treatment of alkyl-substituted aromatic compounds. *Environ.*  
16 868 *Sci. Technol.*, 2020, 54(13):8352-8361.
- 17 869 58. Qian JG, Mopper K, Kieber DJ. Photochemical production of the hydroxyl radical in  
18 870 antarctic waters. *Deep Sea Res. I*, 2001, 48(3):741-759.
- 19 871 59. Gorner H. Photoreduction of 9,10-anthraquinone derivatives, transient spectroscopy and  
20 872 effects of alcohols and amines on reactivity in solution. *Photochem. Photobiol.*, 2003, 77(2):171-  
21 873 179.
- 22 874 60. Gorner H. Photoreduction of p-benzoquinones: Effects of alcohols and amines on the  
23 875 intermediates and reactivities in solution. *Photochem. Photobiol.*, 2003, 78(5):440-448.
- 24 876 61. Gorner H. Photoinduced oxygen uptake for 9,10-anthraquinone in air-saturated aqueous  
25 877 acetonitrile in the presence of formate, alcohols, ascorbic acid or amines. *Photochem. Photobiol.*  
26 878 *Sci.*, 2006, 5(11):1052-1058.
- 27 879 62. Jonsson M, Lind J, Reitberger T, Eriksen TE, Merenyi G. Redox chemistry of substituted  
28 880 benzenes - the one-electron reduction potentials of methoxy-substituted benzene radical cations.  
29 881 *J. Phys. Chem.*, 1993, 97(43):11278-11282.
- 30 882 63. Tafer R, Sleiman M, Boulkamh A, Richard C. Photomineralization of aqueous salicylic  
31 883 acids. Photoproducts characterization and formation of light induced secondary OH precursors  
32 884 (LIS-OH). *Water Res.*, 2016, 106:496-506.
- 33 885 64. Zellner R, Exner M, Herrmann H. Absolute OH quantum yields in the laser photolysis of  
34 886 nitrate, nitrite and dissolved  $\text{H}_2\text{O}_2$  at 308 and 351 nm in the temperature range 278-353 K. *J.*  
35 887 *Atmos. Chem.*, 1990, 10(4):411-425.
- 36 888 65. Sur B, Rolle M, Minero C, Maurino V, Vione D, Brigante M, Mailhot G. Formation of  
37 889 hydroxyl radicals by irradiated 1-nitronaphthalene (1NN): Oxidation of hydroxyl ions and water  
38 890 by the 1NN triplet state. *Photochem. Photobiol. Sci.*, 2011, 10(11):1817-1824.
- 39 891 66. Aeschbacher M, Sander M, Schwarzenbach RP. Novel electrochemical approach to assess  
40 892 the redox properties of humic substances. *Environ. Sci. Technol.*, 2010, 44(1):87-93.
- 41 893 67. Ma JH, Del Vecchio R, Golanoski KS, Boyle ES, Blough NV. Optical properties of humic  
42 894 substances and CDOM: Effects of borohydride reduction. *Environ. Sci. Technol.*, 2010,  
43 895 44(14):5395-5402.
- 44 896 68. Lester Y, Sharpless CM, Mamane H, Linden KG. Production of photooxidants by dissolved  
45 897 organic matter during UV water treatment. *Environ. Sci. Technol.*, 2013, 47(20):11726-33.
- 46 898 69. Berg SM, Whiting QT, Herrli JA, Winkels R, Wammer KH, Remucal CK. The role of  
47 899 dissolved organic matter composition in determining photochemical reactivity at the molecular  
48 900 level. *Environ. Sci. Technol.*, 2019, 53(20):11725-11734.